that the transplanted bone marrow cells can move to damaged muscle and grow into new muscle fibers in mice [24]. Recently, several investigators have reported that transplanted bone marrow cells participate in the muscle regeneration process in irradiated or neonatal recipient mice [25–28]. These procedures opened new pathways for tissue reconstitution therapy via cell transplantation, however, muscle fibers containing donor cell-derived markers were still too low to treat patients with primary myopathies. Very recently, Asakura et al. and others reported the possibility that other muscle stem cells, so-called side population (SP) cells, might exhibit the potential to give rise to myocytes and satellite cells in transplanted muscle [26,29,30]. Thus, the possible interchange among bone marrow cells, muscle SP cells, and satellite cells has received increasing attention from the viewpoint of understanding muscle-specific stem cell biology.

To investigate the molecular events involved in the stimulation and differentiation of satellite cells, it is important to isolate satellite cells from fresh muscles. In this report, we describe the novel monoclonal antibody, SM/C-2.6, that specifically detects satellite cells. SM/C-2.6-positive cells sorted from fresh muscle generated muscle fibers both in vitro and in vivo, and the surface phenotypes of satellite cells were defined.

Materials and methods

Animals and cells

Specific pathogen-free C3H/HeN and C57BL/6 mice aged 6 to 8 weeks were purchased from Charles River Japan (Yokohama, Japan). Specific pathogen-free *mdx* mice (of C57BL/10 background) were provided by Central Laboratories for Experimental Animals (Kanagawa, Japan). C3H/HeN newborn mice were prepared in our animal facility by brother–sister mating. Heterozygous EGFP transgenic (GFP-Tg) mice with a C57BL/6 background [31] were maintained in our animal facility by mating with normal C57BL/6 mice. Sprague–Dawley rats were purchased from CLEA Japan (Tokyo, Japan).

The mouse myogenic cell line C2/4, a subline of C2C12, was a gift from Dr. S. Yoshida (Kyoto University, Kyoto, Japan) and was maintained in culture in 10% FCS containing DMEM medium. A mouse hepatocyte cell line, NCTC1469 [32], was obtained from the Japanese Collection of Research Bioresources, National Institute of Health Sciences, Tokyo, Japan.

Freshly isolated muscle-derived cells from neonatal and adult mice were prepared according to the methods of Rando and Blau [33]. Muscles from neonatal and adult mice were isolated and digested with collagenase type II (Worthington Biochemical Corp., Lakewood, NJ) for 90 min at 37°C. We triturated muscle tissues every 15 min during 90 min incubation and passed through a 37-μm nylon mesh. Single cell suspensions were washed and stained with various mAbs. We usually obtained approximately 5×10^6 cells from 1 g of muscle of 8-week-old female C57BL/6 mice. Sorted cells were obtained from GFP-Tg mice and injected into the tibialis anterior (TA) muscles of *mdx* mice. Two weeks later, the muscles were isolated, frozen in liquid nitrogen-cooled isopentane, and cryosections were examined histologically. Cryosections were examined for GFP^+ muscle fibers under a confocal laser-scanning microscope (model MRC1024ES, Bio-Rad Laboratories, Hercules, CA).

Antibodies

A rat mAb to mouse c-kit (ACK2) [34] was a gift from Dr. S-I. Nishikawa (Kyoto University); it was labeled with FITC in our laboratory. Anti-Sca-1-PE (E13-161.7), anti-CD34-FITC (RAM34), anti-CD45-PE (30-F11), and anti-MyoD (MoAb 5.8A) were purchased from Pharmingen (San Diego, CA). A rabbit anti-mouse M-cadherin polyclonal antibody was prepared in our laboratory. A rabbit anti-mouse laminin polyclonal antibody and TRITC-conjugated goat anti-mouse immunoglobulin were purchased from LSL Co., Ltd. (Tokyo, Japan) and Chemicon International, Inc. (Temecula, CA), respectively. Rhodamine-Red TM-X conjugated goat anti-rabbit IgG and Alexa488-conjugated goat anti-rabbit IgG were purchased from Molecular Probes Inc. (Eugene, OR). A rabbit anti-desmin polyclonal antibody and FITC-conjugated goat anti-rat IgG were purchased from ICN Pharmaceuticals, Inc.-Cappel Products (Aurora, OH). Monoclonal anti-dystrophin (MANDRA-1, Sigma) was labeled with a fluorochrome Alexa 568 in our laboratory. R-PE-streptavidin (Molecular Probes) or FITC-streptavidin (Pharmingen) was used to detect biotinylated antibodies. Anti-human c-met mAb (DO-24) reactive to mouse c-met [35] was purchased from Upstate (Lake Placid, NY), and it was used with Alexa488-conjugated goat anti-mouse IgG (H+L) (Molecular Probes).

Establishment of monoclonal antibodies

MAbs were established according to a standard procedure. Briefly, $1–2 \times 10^6$ C2/4 cells were injected intraperitoneally into Sprague–Dawley rats seven times at weekly intervals. Three days after the last injection, the rats were sacrificed under ether anesthesia and splenocytes were fused with partner cells, P3X63Ag8U.1 (P3U1). Strategies for mAb selection are described in Results. Finally, a mAb clone, SM/C-2.6, was established.

Flow cytometry and cell sorting

Regular flow cytometric profiles were analyzed with a FACSCalibur analyzer and CELLQuest software (Becton Dickinson Immunocytometry Systems, Mountain View, CA). SM/C2.6-reactive mononuclear cells were fractionated on a fluorescent-activated cell sorter (EPICS Elite, Coulter Electronics, Hialeah, FL). Dead cells were excluded from

the plots based on propidium iodide staining (Sigma Co., St. Louis, MO).

Hoechst staining was performed as described by Goodell et al. (http://www.bcm.tmc.edu/genetherapy/goodell/newsite/protocols.html). In brief, hindlimb muscles of 8 week-old C57BL/6 mice were digested with collagenase type II (Worthington Biochemical), suspended at 10^6 cells per ml in Dulbecco's modified Eagle's medium (DME) (Gibco BRL, Grand Island, NY) containing 2% fetal calf serum (FCS, Boehringer-Mannheim GmbH, Mannheim, Germany), 10 mM Hepes, and 5 μg/ml Hoechst 33342 (Sigma), and incubated at 37°C for 90 min in the presence or absence of 50 μM verapamil (Sigma). After Hoechst staining, the cells were washed and stained with biotinylated-SM/C-2.6 and FITC-streptavidin (Pharmingen). Flow cytometric analyses were performed on FACSVantageSE (Becton Dickinson). Hoechst 33342 was excited with a multi-line UV laser (351.1–363.8 nm) and its fluorescence was measured with a 424/44 BP filter and 675/20 BP filter. FITC and PI were excited at 488 nm by an Ar laser, and measured with 530/30 BP and 630/22 BP filters, respectively.

Immunohistochemistry

For immunohistochemical examinations of muscles, cryosections (6 μm) were fixed in acetone for 10 min and incubated in 5% skim milk for 10 min to block nonspecific antibody binding. SM/C-2.6, anti-laminin, anti-M-cadherin, and anti-dystrophin antibodies were applied to the sections for 60 min at 37°C. SM/C-2.6 mAb was detected by FITC-conjugated goat anti-rat IgG as a second antibody. Anti-laminin and anti-M-cadherin antibodies were detected by Rhodamine Red TM-X conjugated goat anti-rabbit IgG. The signals were recorded photographically using an Axiophot microscope (Carl Zeiss, Oberkochen, Germany).

Isolation and immunostaining of single fibers

To detect muscle satellite cells attaching single fibers with SM/C-2.6 and M-cadherin, muscle fibers from extensor digitorium longus (EDL) muscles of C3H/HeN mice were prepared essentially according to the methods of Bischoff [17] and Rosenblatt et al. [18]. Briefly, dissected muscle was incubated with 0.5% type I collagenase (Worthington) in DME at 37°C for 90 min. The muscle mass was transferred to fresh growth medium, high-glucose DME containing 10% FCS and penicillin (200 U/ml)–streptomycin (200 μg/ml) (Gibco BRL). The muscle mass was then triturated with a fire-polished wide-mouth Pasteur pipette. Fibers were transferred to a Matrigel (Collaborative Biomedical, Bedford, MA)-coated Lab-Tek chamber (Nalge Nunc International, Naperville, IL) and fixed in 4% paraformaldehyde in PBS for 5 min at room temperature. Fibers were permeabilized with 0.5% Triton X-100 (Nacalai Tesque, Kyoto, Japan) in PBS at room temperature for 20 min, then the nonspecific binding was blocked by incubation with 5% skim milk (in PBS) for 10 min. SM/C-2.6 and anti-M-cadherin antibodies were applied for 60 min at 37°C. Antibodies were detected using the second antibodies described in the earlier section.

Immunostaining of cultured cells

SM/C-2.6-reactive cells were fractionated on a cell sorter (EPICS Elite, Coulter Electronics), cultured, and then fixed with 2% PFA in PBS at room temperature for 10 min. Cells were permeabilized with 0.25% Triton X-100 in PBS at room temperature and then incubated in 5% skim milk for 10 min. Anti-MyoD and anti-desmin antibodies were added for 60 min at 37°C. Anti-MyoD mAb was detected using TRITC-conjugated goat anti-mouse IgG, and anti-desmin antibody was detected by Alexa 488-conjugated goat anti-rabbit IgG.

Results

Novel monoclonal antibody SM/C-2.6 detects skeletal muscle satellite cells

Satellite cell-specific mAbs were screened in three successive steps. First, mAbs that reacted to C2/4 (C2C12) immunogen were selected by flow cytometry. Second, mAbs that stained mouse thymocytes were discarded to exclude clones reactive to common mouse antigens. At this step, clones reactive to most mouse bone marrow cells were also discarded. Last, the clones reactive to mononuclear cells beneath the basal lamina of mouse skeletal muscles were selected immunohistochemically, and finally, we established the mAb SM/C-2.6. Flow cytometric data show that SM/C-2.6 stains C2/4 (Fig. 1Aa) and a fraction of bone marrow cells (approximately 10%) (Fig. 1Ac), but not thymocytes (Fig. 1Ab). SM/C-2.6 detects mononuclear cells residing beneath the laminin-positive basal lamina of muscle (Figs. 1Ba–c). This is the typical position at which muscle satellite cells reside. SM/C-2.6-positive cells (Fig. 1Bd) were also stained by M-cadherin (Fig. 1Be), which is a typical marker molecule for satellite cells. To confirm that the cells were satellite cells, we isolated living single fibers and stained them with SM/C-2.6. SM/C-2.6-stained mononuclear cells on freshly isolated single fibers. The SM/C-2.6-positive cells attached to a single fiber (Fig. 1Bg) were also stained by M-cadherin (Fig. 1Bh). The myonuclei visualized by counterstaining with DAPI expressed neither SM/C-2.6 nor M-cadherin (Fig. 1Bi).

SM/C-2.6-positive cells differentiate to myoblasts and myotubes in vitro

To determine whether SM/C-2.6-positive cells express other muscle-related molecules, we next fractionated the

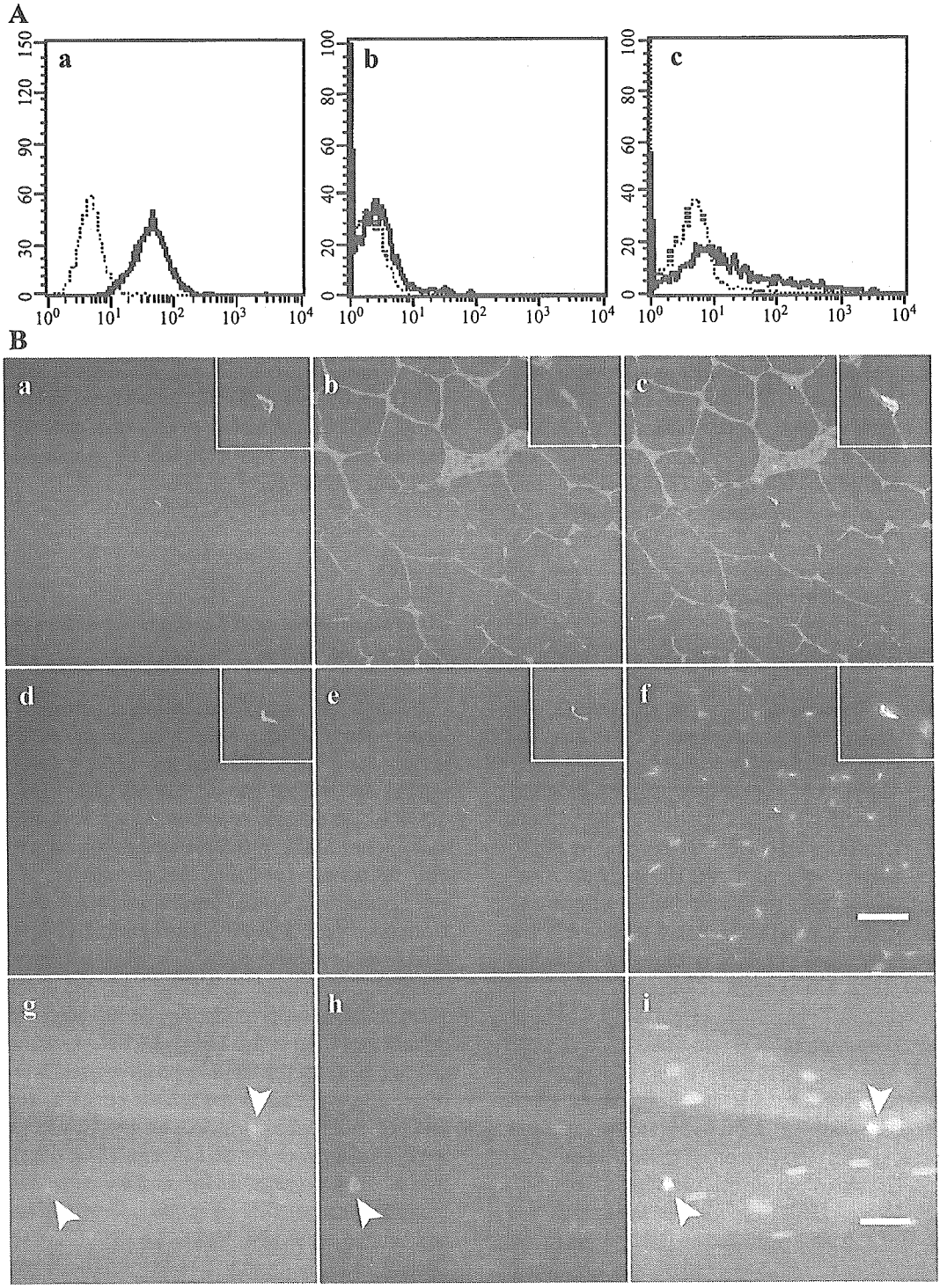

Fig. 1. Establishment of a novel monoclonal antibody, SM/C-2.6. A: SM/C-2.6 reacts with C2/4 cells (a) and a population of bone marrow cells (c), but not with thymocytes (b). Thin lines; control, thick lines; SM/C-2.6. B: Muscle satellite cells were stained with SM/C-2.6. Adult mouse muscle was stained with SM/C-2.6 (a, d), laminin (b), DAPI (c) (merged with a and b), M-cadherin (e), and DAPI (f) (merged with d and e). SM/C-2.6-reactive cells reside beneath the laminin layer and co-stained with anti-M-cadherin antibody. Single fibers from adult EDL muscle were stained with SM/C-2.6 (g), M-cadherin (h), and DAPI (merged with g and h) (i). SM/C-2.6-positive single cells attached to fibers were also stained with M-cadherin. SM/C-2.6 and M-cadherin-positive nuclei are distinguishable from myonuclei (i). Scale bars: 50 μm (a–i).

neonatal mouse muscle-derived mononuclear cells into SM/C-2.6-positive and -negative populations by using FACS sorting and cultured them in vitro. Neonatal muscle contains approximately 25% SM/C-2.6-positive cells (shown later, Fig. 4a). The positively and negatively sorted fractions contain more than 90% and less than 1% SM/C-2.6-positive

cells, respectively (data not shown). After 4 days of proliferating culture, the SM/C-2.6-positive fraction expressed MyoD, a typical myogenic transcription factor (Fig. 2a), while the negative fraction did not (Fig. 2d). The culture medium was then changed to differentiation medium, and the cells were cultured for an additional 7 days and examined for the expression of muscle-related molecules. Many myotubes were formed in the SM/C-2.6-positive fraction and were

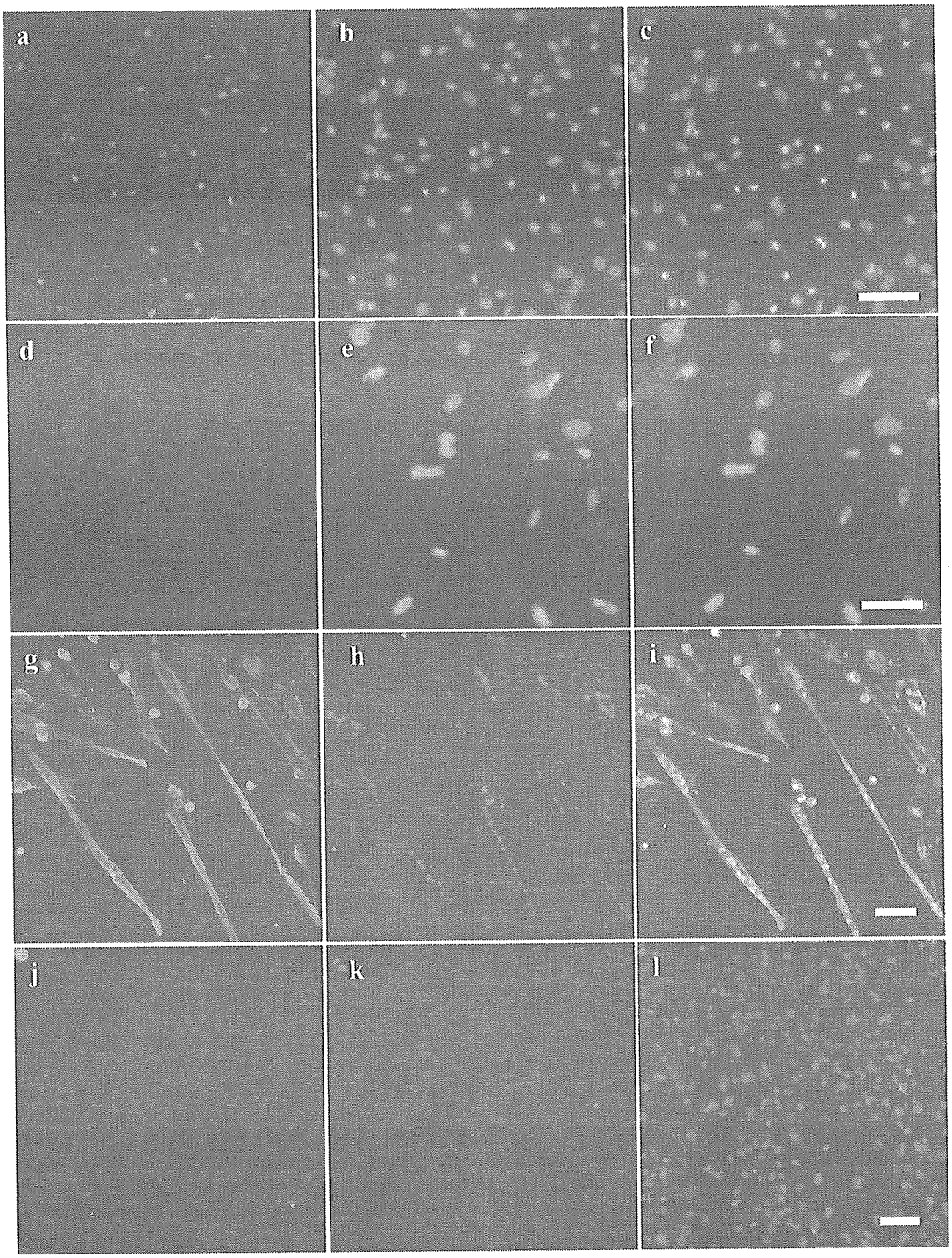

Fig. 2. SM/C-2.6-positive cells differentiate to myotubes in vitro. Freshly isolated single cells from neonatal (day 2) muscles were separated by their reactivity with SM/C-2.6. SM/C-2.6-positive cells compose approximately 25% of the cells in neonatal muscle. The positively and negatively sorted fractions contain 90% and 1% SM/C-2.6-positive cells, respectively. Positively (a–c) and negatively (d–f) sorted cells were cultured for 4 days under proliferating conditions, and the expression of MyoD was determined. Positively sorted cells became MyoD$^+$ (a). b and e; DAPI, c and f; merged. Positively (g–i) and negatively (j–l) sorted cells were then cultured for an additional 7 days under differentiating conditions. Positively sorted cells formed myotubes and became desmin$^+$ (g). Note that lines of MyoD$^+$ myonuclei formed in the newly generated myotubes (h). i and l, merged. Scale bars: 50 μm (a–i).

stained with desmin (Fig. 2g), a muscle-specific intermediate filament protein. MyoD-positive signals formed lines in the satellite cell-derived myonuclei of the myotubes (Fig. 2h), while no such structures were observed in the negative fraction (Figs. 2j–l). These results suggest that SM/C-2.6 specifically detects skeletal muscle satellite cells.

SM/C-2.6-positive cells differentiate into myofibers in vivo

We then examined the satellite cell activity of SM/C-2.6-positive cells in vivo. SM/C-2.6-positive cells were sorted from adult GFP-Tg mice, injected into the TA muscles of *mdx* mice, and the cryosections were examined 2 weeks after transplantation. The SM/C-2.6-positive fraction gave rise to several GFP-positive fibers (Figs. 3a and e), but the negative fraction did not (Figs. 3c and g). Then, we further confirmed that GFP-positive myofibers (Fig. 3i) were positive for dystrophin expression (Figs. 3j and k). Therefore, the SM/C-2.6-positive fraction includes satellite cells.

Age-related changes in SM/C-2.6-positive muscle satellite cells

SM/C-2.6-positive satellite cells were examined in C57BL/6 mice of different ages. Neonatal mice (postnatal day 2) contain approximately 25% satellite cells among the muscular mononuclear cells (Fig. 4a), and this amount declines with age: 13.1% at 4 weeks and 8.9% at 8 weeks of age (Figs. 4b and c). The results agree with earlier studies in which the number of satellite cells was seen to decline with age [13,36–38].

SM/C-2.6 detects neither M-cadherin nor c-met

The antigen recognized by SM/C-2.6 remains to be determined. As shown earlier (Figs. 1Bd and e), SM/C-2.6-positive cells co-express M-cadherin. C2/4 (C2C12) cells express both SM/C-2.6 and M-cadherin (Figs. 5a and b). To investigate whether SM/C-2.6 detects M-cad-

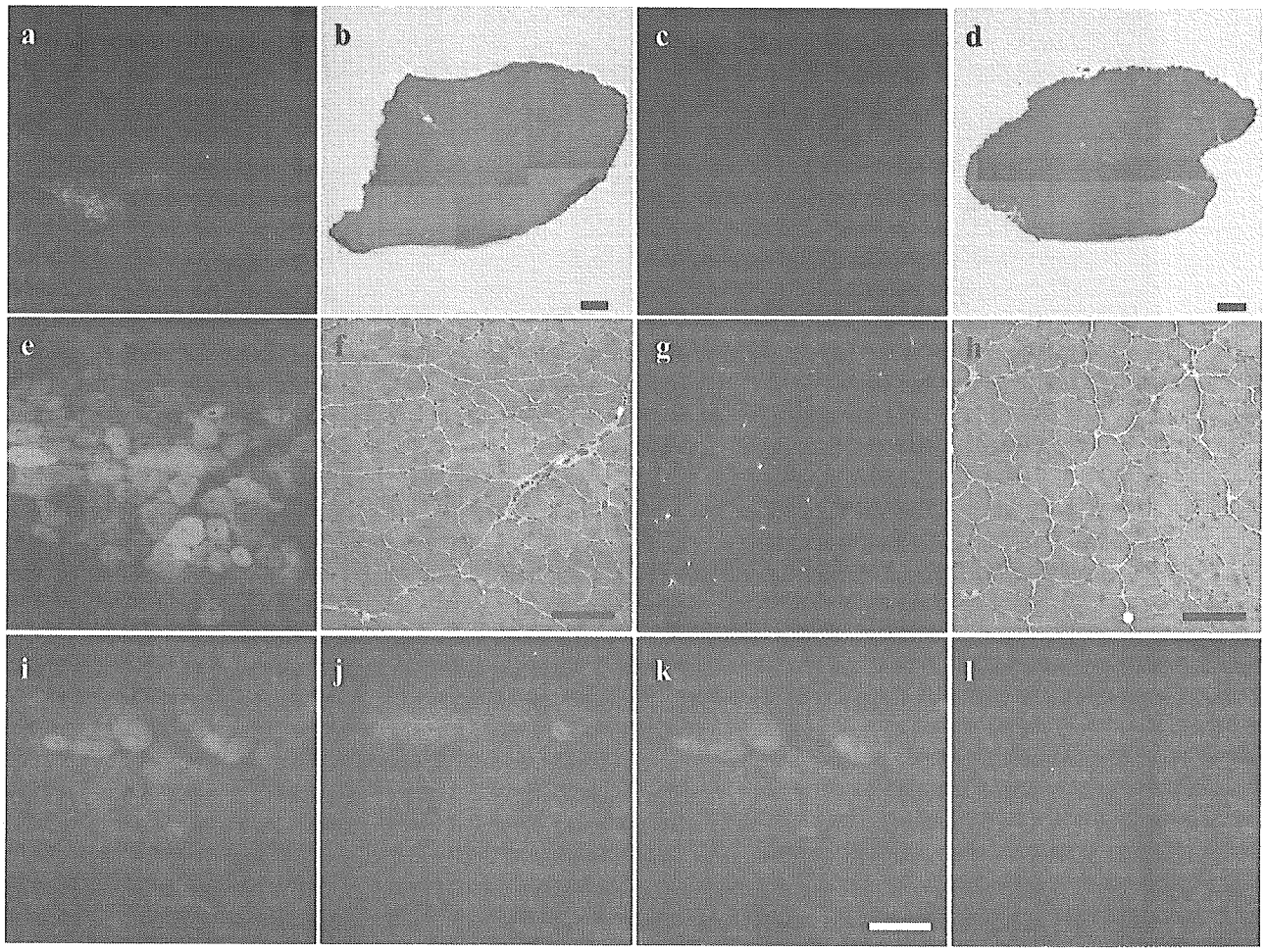

Fig. 3. SM/C-2.6-positive cells differentiate into myofibers in vivo. SM/C-2.6-positive and negative single cells from adult GFP-transgenic mice were obtained by cell sorting, and each muscle cell population was injected intramuscularly into the TA muscles of *mdx* mice. Two weeks later, muscles were isolated and cryosections were examined histologically (GFP: a, c, e, g, i, k; H–E: b, d, f, h). The positive fraction gave rise GFP^+ myofibers (a and e) with central nuclei, whereas the negative fraction did not (c and g). e–h, higher magnifications of a–d. GFP^+-myofibers (i) express dystrophin (j) (k, i and j were merged). GFP-negative area showed no dystrophin expression (l). Scale bars: 250 μm (a–d), and 50 μm (e–l).

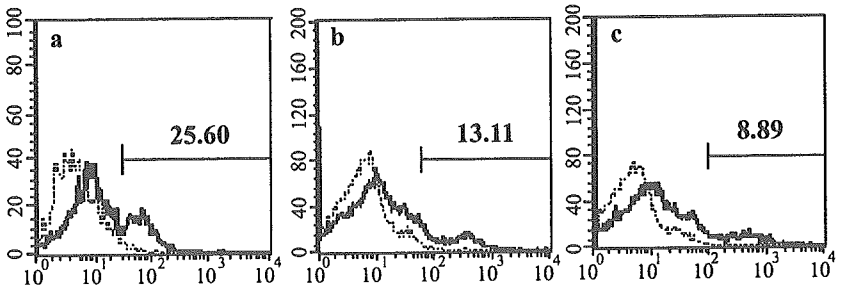

Fig. 4. Age-related changes in SM/C-2.6-positive satellite cells. Flow cytometric analyses of SM/C-2.6-positive cells in the muscles of mice at various ages. SM/C-2.6-positive cells in neonatal (day 2) thigh muscles (a), vastus lateralis and TA muscles from 4-week-old (b) to 8-week-old (c) mice are shown. The numbers of SM/C-2.6-positive cells decreases with age. The gates were set to exclude most of unstained cells. Percentages of unstained cells were equal in all panels.

herin, we compared SM/C-2.6 with M-cadherin expression in bone marrow cells. Approximately 10–15% of bone marrow cells express SM/C-2.6, but there are almost no SM/C-2.6/M-cadherin double positive cells (Fig. 5c). Similar to M-cadherin, we used flow cytometry to compare the expression of c-met and SM/C-2.6-reactive molecules on the mouse hepatocyte cell line NCTC1469. As shown in Fig. 5d, the NCTC1469 clone expresses c-met whereas it does not express SM/C-2.6-reactive molecules. The data definitively indicate that SM/C-2.6 detects neither M-cadherin nor c-met.

SM/C-2.6-positive cells express CD34 but not Sca-1, c-kit, or CD45

To investigate the expressions of several surface marker molecules on SM/C-2.6-positive cells, we analyzed adult muscle-derived mononuclear cells by flow cytometry. SM/C-2.6-positive cells did not co-express Sca-1, c-kit, or CD45 (Figs. 6a–c). However, all SM/C-2.6-positive cells (approximately 10% of muscle-derived mononuclear cells) co-expressed CD34 (Fig. 6d), and significant numbers of $CD34^+$ but SM/C-2.6-negative cells were also found.

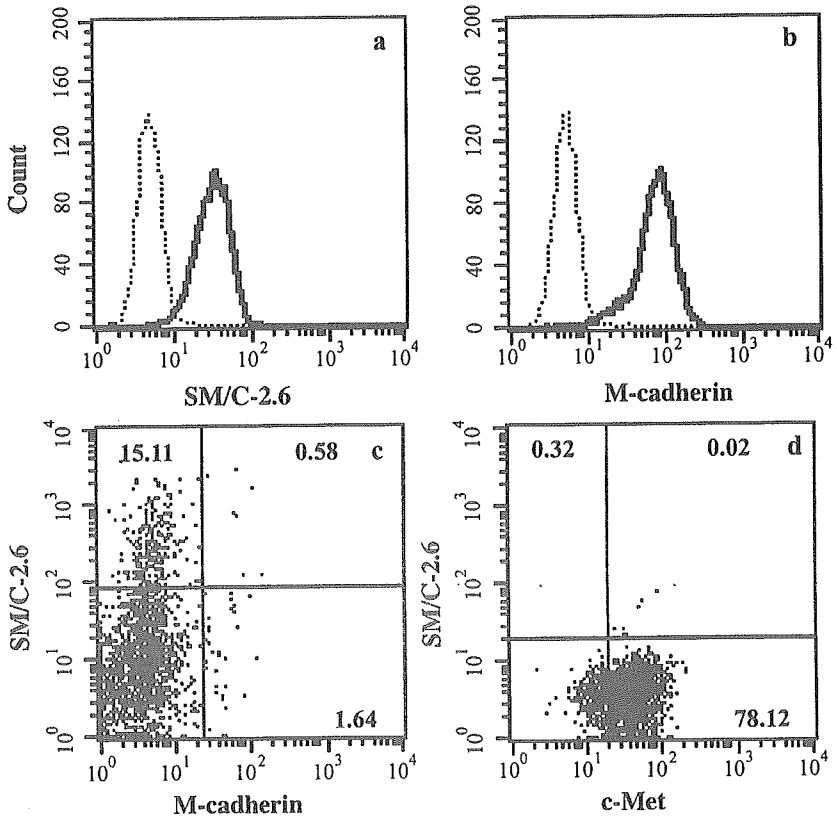

Fig. 5. SM/C-2.6 detects neither M-cadherin nor c-met. The SM/C-2.6-reactive molecule (a, c) and M-cadherin (b, c) are expressed on both C2/4 (a, b) and bone marrow cells (c). Two-color flow cytometry of bone marrow cells showed the SM/C-2.6-positive bone marrow cells do not express M-cadherin. A hepatocyte cell line, NCTC1469, expresses c-met but not the SM/C-2.6-reactive molecule (d). These data indicate that SM/C-2.6 detects neither M-cadherin nor c-met, which are known surface markers of satellite cells.

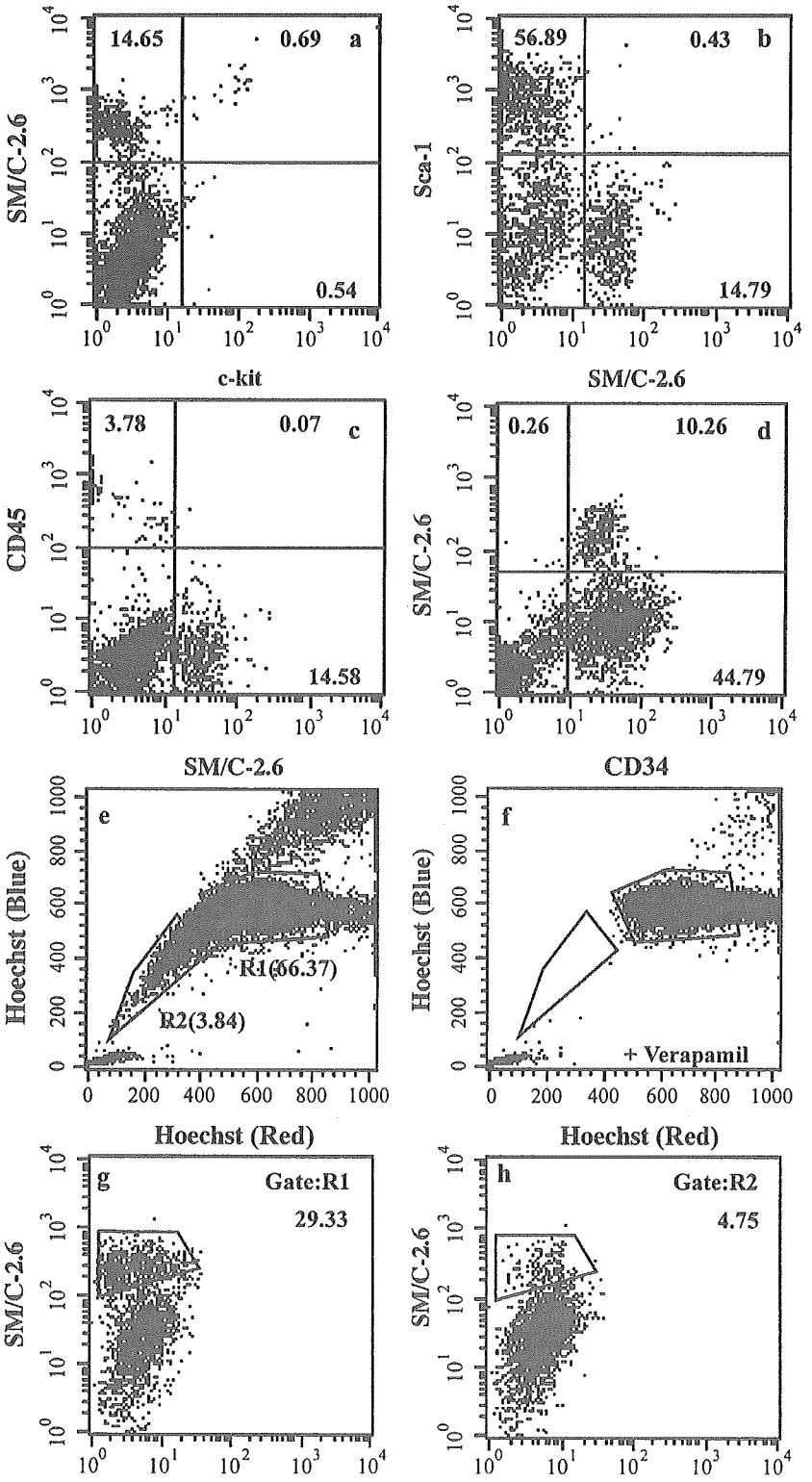

Fig. 6. Satellite cells are Sca-1$^-$, c-kit$^-$, CD45$^-$, CD34$^+$, and are included in the muscle MP fraction. Various surface markers on satellite cells were examined (a–d). SM/C-2.6-positive satellite cells are Sca-1$^-$ (a), c-kit$^-$ (b), CD45$^-$ (c), and CD34$^+$ (d). Muscle SP and MP fractions were separated by FACSVantageSE with (f) or without (e) verapamil. SM/C-2.6-positive cells among SP (3.84%) and MP (66.37%) cells were separated by flow cytometer. MP and SP include 29.33% (g) and 4.75% (h) SM/C-2.6-positive cells, respectively. This suggests that SM/C-2.6-positive satellite cells are mainly included in the muscle MP fraction.

Satellite cells are included in the fraction of muscle main population

Muscle-derived satellite cells can be isolated in the SP fraction by using the Hoechst-dye staining method, and the cells actively participated in myotube formation in the irradiated recipients [26]. Very recently, it was reported that hematopoietic stem cells from muscle SP are of hematopoietic origin [39]. On the other hand, muscle SP cells exhibit the potential to give rise to both myocytes and satellite cells after intramuscular transplantation [29]. We then investigated whether or not the SM/C-2.6-positive cells in adult skeletal muscle are found in the muscle SP fraction. As shown in Fig. 6e, muscle-derived mononuclear cells include 3% SP and a large number of MP cells. The SP fraction disappeared in cells treated with verapamil (Fig. 6f). The MP and SP fractions were gated (Fig. 6e, R1 and R2) and the SM/C-2.6-positive cells were examined. The gated MP fraction contained approximately 30% SM/C-2.6-positive cells (Fig. 6g) but the level was only 5% in the SP fraction (Fig. 6h). The results suggest that satellite cells are mainly included in the MP fraction.

Taken together, the results indicate that skeletal muscle quiescent satellite cells are Sca-1$^-$, c-kit$^-$, and CD45$^-$, but CD34$^+$, and are found in the muscle MP fraction.

Discussion

Muscle satellite cells are known as a key player in the skeletal muscle regeneration. Satellite cells are characterized by several significant features including histological location, electron micrographic characteristics in skeletal muscle, morphological change under physiological or pathological conditions, and the presence of a few specific marker proteins [14]. M-cadherin has been detected in the satellite cells of muscle [40]. Although several methods have been developed to isolate muscle satellite cells from enzymatically digested muscles [17–21], there is no definitive technique to isolate them from fresh muscle. In the present study, we aimed to purify skeletal muscle quiescent satellite cells using a mAb specific for them and to determine the surface phenotype. By immunizing rats with a C2/4 myoblast cell line (a subline of C2C12), we successfully established a novel mAb, SM/C-2.6, that detects muscle satellite cells by immunohistochemical and single fiber methods (Fig. 1B). By using FACS technique, we isolated SM/C-2.6-positive cells from mouse skeletal muscles and demonstrated that these cells differentiated into myotube or muscle fibers both in vivo and in vitro. SM/C-2.6-positive cells were detected in higher numbers in the neonatal muscle (postnatal day 2) than adult (4 week- or 8 week-old). This is consistent with earlier histological observations [14]. As shown in Figs. 2 and 3, FACS-sorted SM/C-2.6-positive cells became desmin$^+$ and MyoD$^+$ under proliferating or differentiating culture conditions. This is in good agreement with earlier studies that showed satellite cells become desmin$^+$ and MyoD$^+$ after muscle injury [41–44] or during short-term culture in vitro [45–47].

M-cadherin expression is restricted to satellite cells postnatally, and it is thought to be one of the proteins that define muscle satellite cells [40]. It is also known that hepatocyte growth factor activates quiescent skeletal muscle satellite cells in vitro [48], and that c-met, a receptor molecule for the factor, is expressed on quiescent satellite cells [49,50]. To investigate whether SM/C-2.6 detects these molecules, we compared the reactivity of SM/C-2.6 with the expressions of c-met in bone marrow cells or in a mouse hepatocyte cell line, NCTC1469. As clearly shown in Fig. 5, SM/C-2.6 detects neither M-cadherin nor c-met. Blanco-Bose et al. [51] reported that α7 integrin was useful for purification of myoblasts from cultured cells. However, α7 integrin is not likely the antigen recognized by SM/C-2.6 because α7 integrin is also expressed on myofibers [52–54]. We are now attempting to identify the reactive molecule.

Gussoni et al. [26] reported that muscle contains hematopoietic stem cells as well as muscle progenitor cells. Although the myogenic potential is highly enriched in muscle MP cells, SP cells with surface markers Sca-1$^+$, Lin$^-$, c-kit$^-$, CD45$^-$, and CD43$^-$, characterized from their efflux of Hoechst dye, are also incorporated into regenerated muscle fibers. The authors showed that the frequency of muscle progenitor cells is much lower than that of hematopoietic cells in muscle SP cells. McKinney-Freeman et al. [39] then showed that Sca-1$^-$ or CD45$^-$ cells give rise to donor-derived muscle fibers when they are injected into mouse muscle. Although it remains controversial, the data suggest that muscle-derived SP cells may not include sufficient muscle satellite cells. Rather, muscle SP cells are mainly composed of hematopoietic stem cells and differentiate into blood cells in the irradiated host. It is possible that they colonize in the muscle and differentiate into muscle satellite cells [29]. As described here, we have found that SM/C-2.6-positive cells in muscle MP cells, while SP cells contain few SM/C-2.6-positive cells. The results suggest that muscle quiescent satellite cells are a different population from SP cells of hematopoietic potential.

Sca-1 and c-kit are well-known surface markers of hematopoietic stem cells [55,56], and CD45 has been found in cells of hematopoietic origin but not on any non-hematopoietic cells [57]. CD34 is also known to be expressed on mouse hematopoietic stem cells [58,59]. As shown here, muscle-derived SM/C-2.6-positive cells do not co-express Sca-1, c-kit, or CD45 (Figs. 6a–c). On the other hand, all SM/C-2.6-positive cells (approximately 10% of muscle-derived mononuclear cells) co-express CD34 (Fig. 6d), and significant numbers of CD34-positive but SM/C-2.6-negative cells are also found. The expression of CD34 on SM/C-2.6-positive satellite cells is in agreement with earlier studies by Beauchamp et al. [60], in which they showed by a single fiber analysis that dormant satellite cells express

CD34 but not Sca-1 or CD45. The authors, however, reported in the paper that approximately 15–20% of satellite cells were negative for CD34 or M-cadherin staining, suggesting heterogeneity of satellite cells. The discrepancy in the CD34 expression on satellite cells remains to be investigated.

Because SM/C-2.6-negative cells give rise to few muscle fibers either in vitro or in vivo (Figs. 2 and 3), we conclude that SM/C-2.6 is a definitive marker of muscle satellite cells, which have the surface markers Sca-1$^-$, c-kit$^-$, CD45$^-$, and CD34$^+$. The characterization of the SM/C-2.6-reactive molecule will provide a powerful tool for understanding muscle-specific stem cell biology and helps us develop cell-base gene therapy or stem cell transplantation therapy for muscular dystrophies.

Acknowledgments

We thank Dr. M. D. Ohto for reading this manuscript. This work is supported by grants-in-aid from the Ministry of Health, Labor and Welfare of Japan.

References

[1] H.L. Aguila, K. Akashi, J. Domen, K. Gandy, E. Lagasse, R.E. Mebius, S. Morrison, J. Shizuru, S. Strober, N. Uchida, D.E. Wright, I.L. Weissman, From stem cells to lymphocytes: biology and transplantation, Immunol. Rev. 157 (1997) 13–40.

[2] H. Nakauchi, K. Sudo, H. Ema, Quantitative assessment of the stem cell self-renewal capacity, Ann. N. Y. Acad. Sci. 938 (2001) 18–24.

[3] R.F. Pereira, K.W. Halford, M.D. O'Hara, D.B. Leeper, B.P. Sokolov, M.D. Pollard, O. Bagasra, D.J. Prockop, Cultured adherent cells from marrow can serve as long-lasting precursor cells for bone, cartilage, and lung in irradiated mice, Proc. Natl. Acad. Sci. U. S. A. 92 (1995) 4857–4861.

[4] D.J. Prockop, Marrow stromal cells as stem cells for nonhematopoietic tissues, Science 276 (1997) 71–74.

[5] M.F. Pittenger, M. Mackay, A.S.C. Beck, R.K. Jaiswal, R. Douglas, J.D. Mosca, M.A. Moorman, D.W. Simonetti, S. Craig, D.R. Marshak, Multilineage potential of adult human mesenchymal stem cells, Science 284 (1999) 143–147.

[6] K.W. Liechty, T.C. MacKenzie, A.F. Shaaban, A. Radu, A.-M.B. Moseley, R. Deans, D.R. Marshak, A.W. Flake, Human mesenchymal stem cells engraft and demonstrate site-specific differentiation after in utero transplantation in sheep, Nat. Med. 6 (2000) 1282–1286.

[7] P. Bianco, P. Gehron-Robey, Marrow stromal stem cells, J. Clin. Invest. 105 (2000) 1663–1668.

[8] S. Makino, K. Fukuda, S. Miyoshi, F. Konishi, H. Kodama, J. Pan, M. Sano, T. Takahashi, S. Hori, H. Abe, J. Hata, A. Umezawa, S. Ogawa, Cardiomyocytes can be generated from marrow stromal cells in vitro, J. Clin. Invest. 103 (1999) 697–705.

[9] A. Erices, P. Conget, J.J. Minguell, Mesenchymal progenitor cells in human umbilical cord blood, Br. J. Haematol. 109 (2000) 235–242.

[10] C. Campagnoli, I.A. Roberts, S. Kumar, P.R. Bennett, I. Bellantuono, N.M. Fisk, Identification of mesenchymal stem/progenitor cells in human first-trimester fetal blood, liver, and bone marrow, Blood 98 (2001) 2396–2402.

[11] Y.A. Romanov, V.A. Svintsitskaya, V.N. Smirnov, Searching for alternative sources of postnatal human mesenchymal stem cells: candidate MSC-like cells from umbilical cord, Stem Cells 21 (2003) 105–110.

[12] A. Mauro, Satellite cells of skeletal muscle fibers, J. Biophys. Biochem. Cytol. 9 (1961) 493–495.

[13] R. Bischoff, The satellite cell and muscle regeneration, in: A.G. Engel, C. Franszini-Armstrong (Eds.), Myogenesis, McGraw-Hill, New York, 1994, pp. 97–118.

[14] M.J. Cullen, Muscle regeneration, in: S.C. Brown, J.A. Lucy (Eds.), Dystrophin: Gene, Protein, and Cell Biology, Cambridge Univ. Press, Cambridge, UK, 1997, pp. 233–273.

[15] M.D. Grounds, Towards understanding skeletal muscle regeneration, Pathol. Res. Pract. 187 (1991) 1–22.

[16] E. Schultz, Satellite cell proliferative compartments in growing skeletal muscles, Dev. Biol. 175 (1996) 84–94.

[17] R. Bischoff, Proliferation of muscle satellite cells on intact myofibers in culture, Dev. Biol. 115 (1986) 129–139.

[18] J.D. Rosenblatt, A.I. Lunt, D.J. Parry, T.A. Partridge, Culturing satellite cells from living single muscle fiber explants, In Vitro Cell. Dev. Biol. Anim. 31 (1995) 773–779.

[19] A. Baroffio, M. Hamann, L. Bernheim, M.L. Bochaton-Piallat, G. Gabbiani, C.R. Bader, Identification of self-renewing myoblasts in the progeny of single human muscle satellite cells, Differentiation 60 (1996) 47–57.

[20] A. Asakura, M. Komaki, M. Rudnicki, Muscle satellite cells are multipotential stem cells that exhibit myogenic, osteogenic, and adipogenic differentiation, Differentiation 68 (2001) 245–253.

[21] Z. Qu-Petersen, B. Deasy, R. Jankowski, M. Ikezawa, J. Cummins, R. Pruchnic, J. Mytinger, B. Cao, C. Gates, A. Wernig, J. Huard, Identification of a novel population of muscle stem cells in mice: potential for muscle regeneration, J. Cell Biol. 157 (2002) 851–864.

[22] S. Wakitani, T. Saito, A.I. Caplan, Myogenic cells derived from rat bone marrow mesenchymal stem cells exposed to 5-azacytidine, Muscle Nerve 18 (1995) 1417–1426.

[23] T. Saito, J.E. Dennis, D.P. Lennon, R.G. Young, A.I. Caplan, Myogenic expression of mesenchymal stem cells within myotubes of *mdx* mice in vitro and in vivo, Tissue Eng. 1 (1995) 327–343.

[24] G. Cossu, F. Mavilio, Myogenic stem cells for the therapy of primary myopathies: wishful thinking or therapeutic perspective? J. Clin. Invest. 105 (2000) 1669–1674.

[25] G. Ferrari, G. Cusella-De Angelis, M. Coletta, E. Paolucci, A. Stornaiuolo, G. Cossu, F. Mavilio, Muscle regeneration by bone marrow-derived myogenic progenitors, Science 279 (1998) 1528–1530.

[26] E. Gussoni, Y. Soneoka, C.D. Strickland, E.A. Buzney, M.K. Khan, A.F. Flint, L.M. Kunkel, R.C. Mulligan, Dystrophin expression in the *mdx* mouse restored by stem cell transplantation, Nature 401 (1999) 390–394.

[27] R.E. Bittner, C. Schofer, K. Weipoltshammer, S. Ivanova, B. Streubel, E. Hauser, M. Freilinger, H. Hoger, A. Elbe-Burger, F. Wachtler, Recruitment of bone-marrow-derived cells by skeletal and cardiac muscle in adult dystrophic *mdx* mice, Anat. Embryol. (Berl.) 199 (1999) 391–396.

[28] S. Fukada, Y. Miyagoe-Suzuki, H. Tsukihara, K. Yuasa, S. Higuchi, S. Ono, K. Tsujikawa, S. Takeda, H. Yamamoto, Muscle regeneration by reconstitution with bone marrow or fetal liver cells from green fluorescent protein-gene transgenic mice, J. Cell Sci. 115 (2002) 1285–1293.

[29] A. Asakura, P. Seale, A. Girgis-Gabardo, M.A. Rudnicki, Myogenic specification of side population cells in skeletal muscle, J. Cell Biol. 159 (2002) 123–134.

[30] T. Tamaki, A. Akatsuka, Y. Okada, Y. Matsuzaki, H. Okano, M. Kimura, Growth and differentiation potential of main- and side-population cells derived from murine skeletal muscle, Exp. Cell Res. 291 (2003) 83–90.

[31] M. Okabe, M. Ikawa, K. Kominami, T. Nakanishi, Y. Nishimune, Green mice' as a source of ubiquitous green cells, FEBS Lett. 407 (1997) 313–319.

[32] G.L. Hobbs, K.K. Sanford, W.R. Earle, V.J. Evans, Establishment of a clone of mouse liver cells from a single isolated cell, J. Natl. Cancer Inst. 18 (1957) 701–707.

[33] T.A. Rando, H.M. Blau, Primary mouse myoblast purification, characterization, and transplantation for cell-mediated gene therapy, J. Cell Biol. 125 (1994) 1275–1287.
[34] S. Nishikawa, M. Kusakabe, K. Yoshinaga, M. Ogawa, S. Hayashi, T. Kunisada, T. Era, T. Sakakura, S.-I. Nishikawa, In utero manipulation of coat color formation by a monoclonal anti-c-kit antibody: two distinct waves of c-kit-dependency during melanocyte development, EMBO J. 10 (1991) 2111–2118.
[35] A. Suzuki, Y. Zheng, S. Kaneko, M. Onodera, K. Fukao, H. Nakauchi, H. Taniguchi, Clonal identification and characterization of self-renewing pluripotent stem cells in the developing liver, J. Cell Biol. 156 (2002) 173–184.
[36] D.R. Campion, The muscle satellite cell: a review, Int. Rev. Cytol. 87 (1984) 225–251.
[37] R. Mazanet, C. Franzini-Armstrong, The satellite cell, in: A.G. Engel, B.Q. Banker (Eds.), Myology, vol. 2. McGraw-Hill, New York, 1986, pp. 285–307.
[38] G. Cossu, M. Molinaro, Cell heterogeneity in the myogenic lineage, Curr. Top. Dev. Biol. 18 (1987) 208–223.
[39] S.L. McKinney-Freeman, K.A. Jackson, F.D. Camargo, G. Ferrari, F. Mavilio, M.A. Goodell, Muscle-derived hematopoietic stem cells are hematopoietic in origin, Proc. Natl. Acad. Sci. U. S. A. 99 (2002) 1341–1346.
[40] A. Irintchev, M. Zeschnigk, A. Starzinski-Powitz, A. Wernig, Expression pattern of M-cadherin in normal, denervated, and regenerating mouse muscles, Dev. Dyn. 199 (1994) 326–337.
[41] T.R. Helliwell, Lectin binding and desmin staining during bupivicaine-induced necrosis and regeneration in rat skeletal muscle, J. Pathol. 155 (1988) 317–326.
[42] Y. Saito, I. Nonaka, Initiation of satellite cell replication in bupivacaine-induced myonecrosis, Acta Neuropathol. 88 (1994) 252–257.
[43] J. Rantanen, T. Hurme, R. Lukka, J. Heino, H. Kalimo, Satellite cell proliferation and the expression of myogenin and desmin in regenerating skeletal muscle: evidence for two different populations of satellite cells, Lab. Invest. 72 (1995) 341–347.
[44] G. Molnar, M.L. Ho, N.A. Schroedl, Evidence for multiple satellite cell populations and a non-myogenic cell type that is regulated differently in regenerating and growing skeletal muscle, Tissue Cell 28 (1996) 547–556.
[45] R.E. Allen, L.L. Rankin, E.A. Greene, L.K. Boxhorn, S.E. Johnson, R.G. Taylor, P.R. Pierce, Desmin is present in proliferating rat muscle satellite cells but not in bovine muscle satellite cells, J. Cell. Physiol. 149 (1991) 525–535.
[46] S.J. Kaufman, M. George-Weinstein, R.F. Foster, In vitro development of precursor cells in the myogenic lineage, Dev. Biol. 146 (1991) 228–238.
[47] S. Creuzet, L. Lescaudron, Z. Li, J. Fontaine-Perus, MyoD, myogenin, and desmin-nls-lacZ transgene emphasize the distinct patterns of satellite cell activation in growth and regeneration, Exp. Cell Res. 243 (1998) 241–253.
[48] R.E. Allen, S.M. Sheehan, R.G. Taylor, T.L. Kendall, G.M. Rice, Hepatocyte growth factor activates quiescent skeletal muscle satellite cells in vitro, J. Cell. Physiol. 165 (1995) 307–312.
[49] D.D. Cornelison, B.J. Wold, Single-cell analysis of regulatory gene expression in quiescent and activated mouse skeletal muscle satellite cells, Dev. Biol. 191 (1997) 270–283.
[50] L.A. Sabourin, A. Girgis-Gabardo, P. Seale, A.A. Sakura, M.A. Rudnicki, Reduced differentiation potential of primary MyoD−/− myogenic cells derived from adult skeletal muscle, J. Cell Biol. 144 (1999) 631–643.
[51] W.E. Blanco-Bose, C.C. Yao, R.H. Kramer, H.M. Blau, Purification of mouse primary myoblasts based on alpha 7 integrin expression, Exp. Cell Res. 265 (2001) 212–220.
[52] W.K. Song, W. Wang, R.F. Foster, D.A. Bielser, S. Kaufman, H36-alpha 7 is a novel integrin alpha chain that is developmentally regulated during skeletal myogenesis, J. Cell Biol. 117 (1992) 643–657.
[53] G. Collo, L. Starr, V. Quaranta, A new isoform of the laminin receptor integrin alpha 7 beta 1 is developmentally regulated in skeletal muscle, J. Biol. Chem. 268 (1993) 19019–19024.
[54] B.L. Ziober, M.P. Vu, N. Waleh, J. Crawford, C.S. Lin, R.H. Kramer, Alternative extracellular and cytoplasmic domains of the integrin alpha 7 subunit are differentially expressed during development, J. Biol. Chem. 268 (1993) 26773–26783.
[55] N. Uchida, I.L. Weissman, Searching for hematopoietic stem cells: evidence that Thy-1.1^{lo} Lin-Sca-1^{+} cells are the only stem cells in C57BL/Ka-Thy-1.1 bone marrow, J. Exp. Med. 175 (1992) 175–184.
[56] M. Osawa, K. Hanada, H. Hamada, H. Nakauchi, Long-term lymphohematopoietic reconstitution by a single CD34-low/negative hematopoietic stem cell, Science. 273 (1996) 242–245.
[57] I.S. Trowbridge, M.L. Thomas, CD45: an emerging role as a protein tyrosine phosphatase required for lymphocyte activation and development, Annu. Rev. Immunol. 12 (1994) 85–116.
[58] D.S. Krause, T. Ito, M.J. Fackler, M. Smith, M.I. Collector, S.J. Sharkis, W.S. May, Characterization of murine CD34, a marker for hematopoietic progenitor and stem cells, Blood 84 (1994) 691–701.
[59] D.S. Krause, M.J. Fackler, C.I. Civin, W.S. May, CD34: structure, biology, and clinical utility, Blood. 87 (1996) 1–13.
[60] J.R. Beauchamp, L. Heslop, D.S. Yu, S. Tajbakhsh, R.G. Kelly, A. Wernig, M.E. Buckingham, T.A. Partridge, P.S. Zammit, Expression of CD34 and Myf5 defines the majority of quiescent adult skeletal muscle satellite cells, J. Cell Biol. 151 (2000) 1221–1234.

Acta Myologica • 2005; XXIV: p. 74-77

Regulation of splicing by MBNL and CELF family of RNA-binding protein

S. ISHIURA*, Y. KINO, Y. NEZU, H. ONISHI, E. OHNO, AND N. SASAGAWA

Department of Life Sciences, Graduate School of Arts and Sciences, The University of Tokyo, 3-8-1 Komaba, Meguro-ku, Tokyo, Japan 153-8902

Myotonic Dystrophy (DM), the most common form of adult-onset muscular dystrophy, comprises at least 2 subtypes, DM1 and DM2. DM1 is caused by the expansion of a CTG repeat located in the 3' untranslated region of the DM protein kinase (*DMPK*) gene. Recently, the expansion of a CCTG tetranucleotide repeat located in the first intron of the *ZNF9* gene was identified as the mutation responsible for DM2. Since both DM1 and DM2 are caused by the expansion of repetitive sequences, some common factors that interact with these sequences might be involved in the pathogenesis of DM. MBNL1 is a candidate for such factors and is thought to be sequestered by the expanded forms of DM transcripts.

Key words: myotonic dystrophy, RNA repeat, MBNL1

Myotonic dystrophy is the most common form of adult-onset muscular dystrophy [1]. It is inherited by autosomal dominant fashion. Myotonic dystrophy causes a consistent constellation of unrelated clinical features, including myotonia, cardiac conduction defects, cataracts, and specific set of endocrine changes, and so on. The underlying genetic mutation causing myotonic dystrophy is unstable expanded CTG repeat in the 3'-untranslated region of a gene on chromosome 19 encoding a DM protein kinase (DMPK) of unknown function [2]. The mutation is transcribed into RNA but not translated into protein. Recently, myotonic dystrophy type 2 (DM2) was found to be caused by a CCTG tetranucleotide expansion in intron 1 of the Zn-finger protein ZNF-9 gene on chromosome 3 [3]. DM2 is also caused by a transcribed but untranslated repeat expansion. Although DM2 is generally a milder disease than DM1, the DM2 CCTG expansions is much larger than DM1 CTG expansions.

Reddy et al. showed that DMPK knockout mice did not fully recapitulate DM. This means that loss of DMPK function is not the main cause of DM [4]. RNA inclusions of CUG/CCUG repeats are observed as foci in the nuclei of DM patients. Transgenic mice expressing CUG repeats under the skeletal muscle actin promoter showed myotonia and abnormal muscle histology [5]. In this case, the severity of phenotype was correlated with the expression level of CUG repeat RNA. These results suggest that abnormality in RNA metabolism is involved in DM [1].

The clinical features common to both DM1 and DM2 may be caused by a gain-of-function RNA mechanism in which the CUG and CCUG repeats alter cellular function by sequestering repeat RNA-binding proteins.

Two families of RNA-binding proteins

Two families of RNA repeat-binding proteins have been implicated in DM pathogenesis: CELF (CUG-BP11 and ETR-3-like factors) and MBNL(muscleblind-like) proteins. Six CELF genes have been identified in human genome and they have been shown to be involved in alternative splicing [6]. Among these, CUG-BP1 regulates alternative splicing of cardiac troponin T (cTnT), insulin receptor (IR) and chloride channel 1 (ClC-1) that are misregulated in DM muscle [7,8]. MBNL is a homologue of *Drosophila* muscleblind which is involved in the differentiation of skeletal muscle and photoreceptor [9]. Three genes (*MBNL1, 2* and *3*) are identified in humans. A mouse knockout reproduced myotonia and cataract, and misregulation of splicing was observed [10].

We investigated the in vivo binding-sequence specificity of these proteins using a yeast 3 hybrid

*Address for correspondence: correspondence should be addressed to Dr. S.Ishiura**

system [11,12]. In this assay, the association of an RNA-binding protein Y with its cognate RNA X binding site leads to the transcriptional activation of a reporter gene, such as His3 and β-galactosidase, in yeast. We generated a variety of repetitive RNA sequences and examined them.

The results are shown in Table 1. CUG-BP1 (this protein is first identified as a CUG triplet repeat-binding protein) strongly interacted with UG dinucleotide repeat [11]. Neither PKR (protein kinase R), a double stranded nucleotide-binding protein, nor CUG-BP1 interacted strongly with CUG/CCUG repeats. By contrast, MBNL1 showed apparent interactions with both CUG and CCUG repeats.

Table 1. RNA-binding specificity of candidate proteins.

Repeat	CUG-BP1	MBNL1	PKR
UG24	+++++	-	-
CA24	-	-	-
CUG7	-	-	-
CUG16	-	++	-
CUG21	-	+++	-
CUG37	-	++	-
CUG70	-	++	+
CCUG7	+	-	-
CCUG22	-	++++	-
CCUG50	-	+++	-
CAGG22	-	-	-
CAGG50	+	-	-
CGGG20	-	-	-
CCCG21	++	++++	-
UAUG7+CAUA7	-	-	+++++
CAG16+CUG16	-	-	+++++

The transformation of yeast cells and reporter gene assays were performed as previously described (11,12). We classified the binding activity as (+++++), (++++), (+++) and (++), when yeast grown was observed on the plates containing 1, 0.5, 0.1 and 0mM 3-AT, respectively. (+) yeast grew in the absence of 3-AT after more than 1 week, (-) no growth of yeast transformants was observed even after prolonged incubation.

We confirmed these results by surface plasmon resonance technique. Surface Plasmon Resonance (SPR) is a powerful technique to measure biomolecular interactions in real-time in a label free environment. Protein is immobilized to the sensor surface, and the repeat RNA is passed over the surface. Association and dissociation is measured and displayed in a graph called the sensor-gram. CUG-BP1 strongly interacted with UG-repeat but not CUG repeat, while MBNL1 interacted with CCUG repeat (data not shown). These results indicate that loss of function of MBNL1, not CUG-BP1, may be important for DM pathogenesis. Sequestration of MBNL1 by the long CUG/CCUG repeat may disrupt normal cellular function of MBNL1, which leads to abnormal phenotype of myotonic dystrophy.

Table 1 also shows that MBNL1 interacted strongly with CCCG, modestly with CUUG and CAUG, but not at all with CGGG and so on. On the other hand, PKR strongly interacted with double-stranded RNAs. All these results suggest MBNL1 binds to repeats with incomplete double strand, but not to the complete one. The deduced target sequence of MBNL1 could be CHHG or CHG repeat, where H is the nucleotide other than G. Secondary structure of CHHG repeat can be calculated as a long hairpin with mismatches. Since MBNL1 does not bind to CUG/CAG double strand repeat without mismatch, the presence of mismatch is necessary for the binding of MBNL1 to the target sequences.

To confirm the results of the three-hybrid analyses, we performed gel retardation analysis [12]. First, we fused MBNL1 with glutathione S-transferase (GST) in the N-terminus and a His-tag in the C-terminus. GST-MBNL1 was expressed in E.Coli and purified. GST-MBNL1 bound to a ^{32}P-labeled CCUG probe, and supershift was observed when an anti-GST antibody was added. The extent of band shift was reduced by adding non-labeled CCUG RNA. We also examined the dependence of the binding between CCUG repeats and MBNL1 on the repeat length. Free probes of CCUG27 and CCUG35 disappeared at the highest dose of MBNL1. The number of shifted bands represents the variety of RNA-protein complexes, mainly reflecting the number of proteins binding to a single probe.

Structure of MBNL1 and homologues

MBNL1 has at least nine splice variants. MBNL1 has four Zn finger motifs at the N-terminal half of the molecule, which may be involved in the RNA-binding. There is a nuclear localization signal at the C-terminus. Some of the isoforms of MBNL1 was localized at the nucleus. The others were in the cytosol. Therefore, MBNL1 might have many cellular functions. Furthermore, not only MBNL1 but also MBNL2 and 3 are

reported to be colocalized with RNA foci of CUG/CCUG repeats. We have determined the binding specificity of these MBNL families to various RNA repeats. MBNL2 and MBNL3 had almost similar specificity to MBNL1 (data not shown). These MBNL isoforms also showed different localization. Therefore we have to be careful for analyzing the data, because three MBNL proteins have many isoforms and these isoforms may have diverse functions in various tissues.

Regulation of alternative splicing by RNA repeat-binding proteins

Myotonic dystrophy is an example of a disease that alters the function of RNA-binding proteins to cause misregulated alternative splicing [1]. Many misregulated alternative splicing events have been demonstrated for eight pre mRNAs. In all cases, normal mRNA splice variants are produced, but the normal developmental splicing pattern is disrupted, resulting in the expression of fetal protein isoforms.

The insulin resistance and myotonia observed in DM1 correlate with the disruption of splicing of targets, IR and ClC-1. The counter regulation of mRNA splicing by the two proteins, CUG-BP1 and MBNL1 is demonstrated [9]. When cTNT mini-gene was expressed with CUG-BP1, a fetal isoform including exon 5 was predominantly expressed, while coexpression with MNBL1 suppressed the formation of the fetal isoform. In the case of insulin receptor mini-gene, MBNL1 enhanced the formation of long form with exon 11, while CUG-BP1 was not. These results suggest that these two RNA-binding proteins counteracted *in vivo*.

However, in the case of alpha-actinin, MBNL1 may not always act antagonistically against CUG-BP1s. Alpha-actinin has two exons, nonmuscle type and skeletal muscle type. These are exclusively expressed in vivo. However, in our assay system, MBNL1 does not act antagonistically against CUG-BP1. Both enhanced the production of non-muscle type (Fig.1). These data also predict that change in expression of these alternative splicing regulators would result in the splicing alterations that have been shown to be characteristic of the myotonic dystrophy. However, all targets of these proteins have never been clarified. In addition, these regulators appear to express independently.

There have been many reports that excess oxidative stress occurs in the muscle with expanded CTG repeats [13-15]. The stress accelerates an apoptotic process, leading to cell death. The increase in oxidative stress in response to expended RNA repeats is likely to involve yet unidentified signaling event that remain to be determined. Misregulation of splicing may also be evoked by the cellular signaling processes.

Acknowledgments

This work was supported in part by grants (to S.I.) from the Ministry of Health, Labor and Welfare, Japan, and the Ministry of Education, Science, Sports and Cuture, Japan.

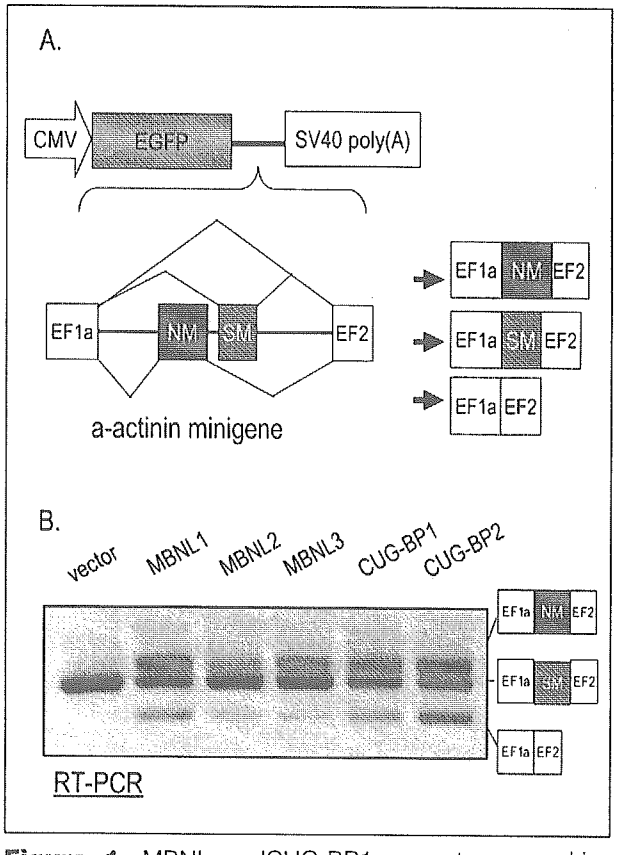

Figure 1. MBNL andCUG-BP1 promote exon skipping.

A. The α-actinin minigene contains two exons (nonmuscle type NM and smooth muscle type SM) flanked by EF1a and EF2 exons.

B. COS cells were cotransfected with the minigene and each of RNA-binding protein expression plasmid. Exon inclusion was assayed by RT-PCR.

References

1. Ranum LPW, Day JW. Myotonic dystrophy:RNA pathogenesis comes into focus. Am J Hum Genet 2004;74:793-804.
2. Sasagawa N, Ishiura S. Myotonic dystrophy protein kinase. Wiley Encyclopedia Mol Med 2002;5:2203-05.
3. Day JW, Ricker K, Jacobson JF, et al. Myotonic dystrophy type 2:molecular, diagnostic and clinical spectrum. Neurology 2003;60:657-64.
4. Reddy S, Smith DB, Rich MM, et al. Mice lacking the myotonic dystrophy protein kinase develop a late onset progressive myopathy. Nat Genet 1996;13:325-335.
5. Ladd AN, Nguyen NH, Malhotra K, Cooper TA. CELF6, a member of the CELF family of RNA-binding proteins, regulates muscle-specific enhancer-dependent alternative splicing. J Biol Chem 2004;279:17756-64.
6. Mankodi A, Logigian E, Callahan L, et al. Myotonic dystrophy in transgenic mice expressing an enpanded CUG repeat. Science 2000;289:1769-73.
7. Timchenko LT, Timchenko NA, Caskey CT, Roberts R. Novel proteins with binding specificity for DNA CTG repeats and RNA CUG repeats: implication for myotonic dystrophy. Hum Mol Genet 1996;5:1115-21.
8. Ho TH, Bundman D, Armstrong DL, Cooper TA. Transgenic mice expressing CUG-BP11 reproduce splicing mis-regulation observed in myotonic dystrophy. Hum Mol Genet 2005;14:1539-47.
9. Ho TH, Charet-B N, Poulos MG, et al. Muscleblind proteins regulate alternative splicing. EMBO J 2004;23:3103-12.
10. Kanadia RN, Johnstone KA, Mankodi A, et al. A muscleblind knockout model for myotonic dystrophy. Science 2003;302:1978-80.
11. Takahashi N, Sasagawa N, Suzuki K, Ishiura S. The CUG-binding protein (CUG-BP1) binds specifically to UG dinucleotide repeats in a yeast three-hybrid system. Biochem Biophys Res Commun 2000;277:518-23.
12. Kino Y, Oma Y, Sasagawa N, Ishiura S. Muscleblind protein, MBNL1/EXP, binds specifically to CHHG repeats. Human Mol Genet 2004;13:495-507.
13. Usuki F, Takahashi N, Sasagawa N, Ishiura S. Differential signaling pathways following oxidative stress in mutant myotonin protein kinase cDNA transfected C2C12 cell lines. Biochem Biophys Res Commun 2000;267:739-743.
14. Usuki F, Yasutake A, Umehara F, et al. In vivo protection of a water-soluble derivative of vitamin E, Trolox, against methylmercury-intoxication in the rat. Neurosci Lett 2001;304:199-203.
15. Takeshita Y, Sasagawa N, Usuki F, Ishiura S. Decreased expression of alpha-B-crystallin in C2C12 cells that express human DMPK/160CTG repeats. Basic Appl Myol 2003;13:305-8.

Available online at www.sciencedirect.com
SCIENCE DIRECT®
Neuroscience Research 49 (2004) 47–54
Neuroscience Research
www.elsevier.com/locate/neures

Altered expression of CUG binding protein 1 mRNA in myotonic dystrophy 1: possible RNA–RNA interaction

Tomoji Watanabe[a,*], Akio Takagi[a], Noboru Sasagawa[b], Shoichi Ishiura[b], Hirofumi Nakase[a]

[a] *Department of Neurology, Toranomon Hospital and Okinaka Memorial Institute for Medical Research, 222 Toranomon, Minato-ku, Tokyo 105-0001, Japan*

[b] *Department of Life and Cognitive Sciences, College of Arts and Sciences, The University of Tokyo, 381 Komaba, Meguro-ku, Tokyo 153-8902, Japan*

Received 4 November 2003; accepted 20 January 2004

Abstract

The triplet repeats mutation, which causes myotonic dystrophy 1 (DM1), is thought to have a dominant negative effect on RNA levels. In light of previous results using differential display analysis, the present study focused on the expression of CUG binding protein 1 (CUGBP1) mRNA. Northern blot analysis demonstrated that the quantity of CUGBP1 mRNA in three DM1 patients was approximately 70% of that observed in three normal controls ($P < 0.05$). In addition, a semi-quantitative RT-PCR assay showed that the relative amount of CUGBP1 mRNA was reduced in muscle biopsy samples from 10 DM1 patients compared to that from five normal individuals ($P < 0.01$) and 10 myopathic disease controls ($P < 0.01$). The amount of CUGBP1 mRNA was negatively correlated with the size of the CTG expansion ($r = -0.85$, $P < 0.05$). In vitro RNA–RNA binding experiments demonstrated that the incubation of expanded CUG repeats with CUGBP1 RNA generated a higher molecular weight band, which was digested by RNase III. The CUGBP1 mRNA was found to contain several CAG repeat sequences. These results suggest that the CUG expansion may bind to complementary sequences within the CUGBP1 mRNA and that this molecular interaction may affect CUGBP1 mRNA expression in DM1.

Keywords: Myotonic dystrophy (DM); CTG repeat; CUG binding protein (CUGBP); DM protein kinase (DMPK); mRNA; RNA–RNA interaction

1. Introduction

Myotonic dystrophy 1 (DM1) is a multi-system disorder that is characterized by myotonia and progressive muscle weakness. Patients with DM1 have a large number of CTG triplet repeats in the 3′-untranslated region of the DM protein kinase (DMPK) gene, which has been mapped to chromosome 19q 13.3. The length of the CTG triplet repeats correlates well with the age of onset and severity of the disease (Harley et al., 1992).

The mechanisms that a non-translated CTG repeat in a single allele results in the severe dominant phenotype of DM1 remains unclear. One possible explanation is that this series of repeats may disrupt the expression of other genes at either the DNA or RNA level (Harris et al., 1996). The repeat expansion has been identified as a *cis*-acting determinant, which affects neighboring genes (Thornton et al., 1997; Klesert et al., 1997). Another hypothesis is that a triplet expansion in the 3'UTR of the DMPK gene may affect the expression of other mRNAs. Several studies have suggested that the DM1 mutation has a *trans*-effect on cellular RNA expression (Sabourin et al., 1997; Sasagawa et al., 1999; Amack et al., 1999).

Here, we screened mRNAs expressed in DM1 muscle using fluorescent differential display analysis, which has been used to detect differentially expressed genes (Liang and Pardee, 1992). CUGBP1 mRNA has been shown to be differentially expressed in patients with DM1. The product of CUGBP mRNA is one of a family of RNA binding proteins. While the biological function of CUGBP has not yet been established, it is speculated that (CUG)n repeat region in DMPK mRNA is a binding site for the CUGBP protein, and triplet repeat expansion leads to sequestration of this protein on mutant DMPK transcript (Timchenko et al., 1996). Recent report proposed that CUGBP might cause disruption of alternative splicing of pre-mRNA of muscle specific

* Corresponding author. Tel.: +81-3-3588-1111; fax: +81-3-3582-7068.
E-mail address: watanabe-t@toranomon.gr.jp (T. Watanabe).

0168-0102/$ – see front matter © 2004 Elsevier Ireland Ltd and The Japan Neuroscience Society. All rights reserved.
doi:10.1016/j.neures.2004.01.008

chloride channel in DM1 (Charlet et al., 2002). In the present study, we hypothesized alteration of CUGBP mRNA might be involved in a *trans*-RNA interaction between CUG repeats and CUGBP1 mRNA. Therefore, we performed an in vitro RNA–RNA binding assay to examine this hypothesis.

2. Materials and methods

2.1. Muscle biopsy, total RNA preparation and cDNA synthesis

Twenty-five open biopsied samples of biceps muscle from 10 DM1 patients (mean age ± S.D., 32.6 ± 5.6 years, seven men and three women), 10 myopathic disease controls (5 limb-girdle muscular dystrophy, three distal myopathy and two facioscapulohumeral muscular dystrophy patients, 29.1 ± 7.9 years, six men and four women), and five normal individuals (33.3 ± 2.6 years, three men and two women) who exhibited no pathological findings were analyzed. Written, informed consent was obtained from all subjects or their parents before biopsy. All samples were immediately frozen in liquid nitrogen after biopsy and were stored at −70 °C until analysis. Total RNA was prepared from the biopsies by the guanidinium–HCl/thiocyanate/phenol/chloroform method. To remove any contaminating DNA, the RNA was treated with DNase 1 (TaKaRa, Tokyo, Japan) for 30 min at 37 °C. After acid phenol extraction and isopropanol precipitation, 1 μg of DNA-free total RNA was placed in 8 μl of DEPC-treated water. The solution was heated to 65 °C for 10 min, and then cooled to 37 °C. To this solution was added 15 mM DTT, 1.8 mM of each dNTP, 1 μM of the appropriate primers, and 5 U of reverse transcriptase (Amersham Pharmacia Biotech, UK).

2.2. Southern blot analysis

Peripheral blood leukocytes were prepared for extraction of DNA for Southern blot analysis from all of the DM1 patients and one normal individual. For detection of mutant alleles, 10 μg per lane of *Bam*HI restriction fragments were resolved by electrophoresis on a 1.0% agarose gel and were transferred to Hybond-N+ nylon membranes (Amersham Pharmacia Biotech). The primer set for amplification of the 3′ end of the human DMPK gene, not including the repeat region, was designed as follows: Forward: 5′-CAC GGA TCC ACC TTC CCA TG-3′ (corresponding to nucleotides 9568-9587); Reverse: 5′-CCA TCT AGC TGG AGA GAG AA-3′ (9864–9883). The 316 bp PCR product, which was subcloned into the PUC118 cloning vector (Takara) and labeled with [^{32}P]dCTP using a Megaprime DNA Labeling Kit (Amersham Pharmacia Biotech), was used as the DNA probe. The bands were visualized using a BAS 2000 Image Analyzer (Fuji Medical Systems, Stanford, USA).

2.3. Fluorescent differential display analysis

Fluorescent differential display analysis was performed using RNA prepared from biopsied skeletal muscles taken from three DM patients and three normal control individuals. Conditions for the experiment have been described previously (Watanabe et al., 1999). Briefly, three fluorescein isothiocyanate (FITC)-labeled 3′-anchored oligo (d)T primers (FITC-5′-CGTACGCGT$_{15}$N-3′, where N = one of A, C or G) and 60 arbitrary primers were used for PCR. Isomigrating bands, which were amplified to a different degree depending upon whether the sample came from a patient or control individual, were excised and re-amplified using the same set of primers. The re-amplified bands were subcloned into the pT7Blue-cloning vector (Novagen) and fully sequenced in both directions. Comparison studies were performed using the GenBank database of the National Center for Biotechnology Information (Bethesda, MD, USA). Subcloned bands of interest were used as probes for Northern blot analysis, and labeled with [^{32}P] dCTP using a Megaprime DNA Labeling Kit (Amersham Pharmacia Biotech). For standardization of lane loading differences, membranes were subsequently hybridized with a probe specific for human β-actin. The bands were visualized using a BAS 2000 Image Analyzer (Fuji Medical Systems).

2.4. Semi-quantitative multiplex PCR assay

For quantitative analysis of CUGBP1 mRNA, a semi-quantitative multiplex RT-PCR assay was developed. Primer sequences were as follows: CUGBP1, Forward: 5′-AAC AAT GCA GTG GAA GAC AGG-3′ (corresponding to nucleotides 441–460), Reverse: 5′-CTC CAG CTA ATG TCT GCA GG-3′ (1076–1095); β-actin (internal control), Forward: 5′-CTA CAA TGA GCT GCG TGT GG-3′ (343–362), Reverse: 5′-CAT ACT CCT GCT TGC TGA TCC-3′ (1040–1060). PCR using these amplimers yielded PCR products of 655 bp and 818 bp, respectively. The reaction volume was 20 μl and contained 1 μl of cDNA solution, 10x PCR buffer, 0.25 mM of each dNTP, 0.5 μM each of the forward and backward primers, and 0.5 U of Ex Taq DNA polymerase. Initially, we defined the kinetics of co-amplification of the CUGBP1- and β-actin-specific PCR products using normal control samples. PCR was performed as follows: denaturation at 94 °C for 1 min for 1 cycle; then 18 to 23 cycles each of denaturation at 94 °C for 15 s, annealing at 57 °C for 1 min, and elongation at 74 °C for 3 min. The reactions were amplified through 21 cycles. The reactions were sampled after every cycle, resolved by electrophoresis on a 5% polyacrylamide sequencing gel, and the bands were stained with SYBR Green I (TaKaRa). The intensity of SYBR Green I luminescence was measured using a FluoroImager scanner (Molecular Dynamics) and was analyzed with ImageQuant software (Molecular Dynamics). It was demonstrated that reaction cycle-intensity curves fit the linear portion of

semi-logarithmic graphs from 18 to 22 cycles of reaction, and both CUGBP1- and β-actin-specific PCR products were presumed to be amplified with comparable efficiency under these conditions (Fig. 2A and B). Thus, we examined the level of expression of the mRNAs in all biopsied samples using a quantitative multiplex RT-PCR assay, as described above.

2.5. Binding of CUG repeat to CUGBP1 RNA in vitro

Fluorescein 12-UTP-labeled single strand riboprobes were generated from cloned human DMPK, CUGBP1 and β-actin cDNAs. Primer sequences to amplify DMPK cDNA were as follows: Forward: 5′-CCT AGA ACT GTC TTC GAC TCC G-3′ (corresponding to nucleotides 2669–2690), Reverse: 5′-TTG CGA ACC AAC GAT AGG TGG G-3′ (3040–3061). Primers for CUGBP1 and β-actin were identical to those used for the quantitative multiplex PCR described above. The amplified 655 and 818 bp products were subcloned into the pT7 Blue T-vector (Novagen, Madison, USA), while those for DMPK amplified 374 bp (one of normal individuals) and 518 bp (one of DM1 cases) products containing 12 and 60 CTG repeats respectively were subcloned into the pSPT18 vector (Boehringer Mannheim GmbH Biochemica, Mannheim, Germany). The CUGBP1 cDNA was cleaved with Ear I (position 591 and 778) and AlwNI (position 836) into three fragments, named R1 (187 bp), R2 (58 bp) and R3 (259 bp). The fragments were re-ligated (Fig. 3A). All subcloned cDNAs were linearized, and sense and anti-sense riboprobes were transcribed in vitro by a RNA labeling kit (Boehringer Mannheim) using T7 or SP6 RNA polymerases and were concentrated to 20 pM. Each combination of riboprobe was incubated in 20 μl of standard binding buffer (Tomizawa, 1985) containing 10 mM $MgCl_2$ and 100 mM NaCl in 20 mM Tris-HCl (pH 7.6) at 70 °C for 3 min in the same tubes, followed by slow cooling at 4 °C, as previously described (Skripkin et al., 1996; Besancon and Wagner, 1999). Some of reactions were incubated with 0.0001, 0.001 or 0.01 Unit RNase III (Epicentre Technologies, Wisconsin, USA) at 37 °C for 15 min. Samples were analyzed by 1% agarose gel electrophoresis, and scanned with the FluoroImager machine (Molecular Dynamics) at the high sensitive mode.

2.6. Statistics

Since the sample groups were small, comparisons between the relative levels of the mRNAs and proteins in DM1 patient tissues versus controls were performed using the non-parametric Mann–Whitney test. Correlations between the CTG-repeat size and the relative amount of the mRNAs and proteins in DM1 patients were expressed as Pearson's correlation coefficients. Significance was set at $P < 0.05$ in all tests.

3. Results

3.1. CTG expansion in DM1 patients

The normal BamH1 fragment of 1376 bp was observed in the control WBCs, while the expanded allele, varying between approximately 1760 and 5540 bp, was identified exclusively in DM1 patients. Thus, the number of triplet nucleotide repeats was calculated to range from 128 to 1388. Fig. 1A shows representative triplet repeats of 1388, 1229, and 128 in lanes 1, 2, and 3, respectively.

3.2. Decreased level of CUGBP1 mRNAs expression in DM1 biopsies

One PCR product was differentially amplified between the two samples (Fig. 1B). This product, which was expressed to a lesser degree in the DM1 patients than in normal controls, was identical to Homo sapiens CUGBP1 mRNA (Accession no. U63289). Northern blot analysis showed that the quantity of CUGBP1 mRNA in the controls was approximately 113% greater than that of the affected individuals ($P < 0.05$) (Fig. 1C and D).

The RT-PCR based assay was performed on biopsied muscle samples from 10 DM1 patients, 10 myopathy controls and five normal individuals. Fig. 2C shows a representative analysis of the tissue expression levels of CUGBP1 and β-actin mRNAs. In DM1 muscle biopsies, the ratio of CUGBP1 to β-actin band density was significantly greater than in the myopathy controls ($P < 0.01$) and normal controls ($P < 0.01$) (Fig. 2D). There was no significant difference between the myopathy controls and normal individuals ($p = 0.378$) (Fig. 2D). In DM1 patients, the number of CTG repeats negatively correlated with the ratio of CUGBP1 to β-actin band density ($r = -0.85$, $P < 0.05$) (Fig. 2E).

3.3. The CUG expansion binds to CAG repeats within CUGBP1 mRNA in vitro

The primers for CUGBP1 cDNA were designed to amplify a partial ORF of the 655 bp product, which has 32 CAG trinucleotides containing five of (CAG)2 and 1 of (CAG)3. A quarter of the CAG trinucleotides are located within nucleotide 778–836 (Fig. 3A). Thus, we assessed the anti-sense binding of the CUG repeats to the complementary sequence in CUGBP1 mRNA. Initially we generated fluorescein 12-UTP-labeled riboprobes comprising (CUG)12, (CAG)12, (CUG)60 or (CAG)60. Fig. 3B demonstrates that the incubation of (CUG)60 with (CAG)12, as well as with (CAG)60 produced a band shift, which was slightly observed in the incubation of (CUG)12 with (CAG)12. On the other hand, (CAG)12 showed almost identical migration to that of (CAG)60, even though both has significantly different length. This was also seen in (CUG)12 and (CUG)60. It was suggested that (CAG)60 or (CUG)60 formed secondary structure to increase migration to migrate in the

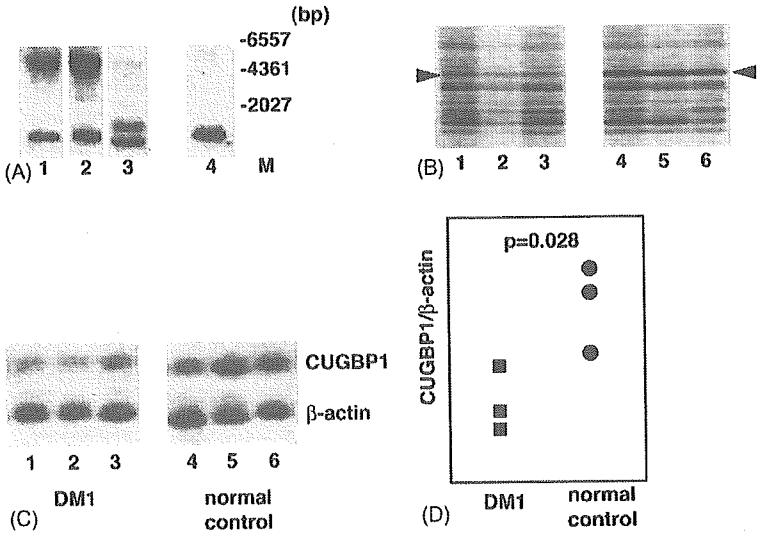

Fig. 1. (A) Measurement of the size of the CTG expansion. The DNA probe, which was 316 bp in size, was labeled with [^{32}P] dCTP and was used for Southern blot analysis. The BamH1 fragment from the normal allele is 1376 bp in size (lane 4), while an additional larger band, varying between approximately 2500 and 11 000 bp, is identified in DM patients (lanes 1–3). M: size marker. (B) Differentially expressed clones. Lanes 1–3: DM patients; lanes 4–6: normal controls. The band indicated by the arrowhead is amplified to a lesser degree in DM patients than in the controls. This PCR product was excised from the gel, subcloned into a plasmid vector and then sequenced. The sequence of the subclone was 100% identical to that of CUGBP1. (C, D) Northern blot analysis of the CUG binding protein 1 mRNA. Lanes 1–3: DM patients; lanes 4–6: normal controls. The differentially amplified PCR product, identified as CUGBP1 mRNA, was labeled and hybridized with total RNA (15 μg loaded/lane) from biopsied muscle samples. β-Actin mRNA is included at the bottom of the figure to control for RNA loading (C). The data show that the quantity of CUGBP1 mRNA in the controls is approximately 113% greater than that in DM patients (D).

position almost identical to that of (CAG)12 or (CUG)12. Next, we generated CUGBP1 sense and anti-sense RNAs and incubated these with the CUG repeats. Fig. 3C shows that CUGBP1 sense RNA hybridized with (CUG)60 RNA, while no band shift was found after the incubation of CUGBP1 anti-sense RNA with (CUG)60 RNA. In addition, β-actin RNA containing no CAG repeats did not interact with (CUG)60 RNA. To identify the binding site, three truncated forms of CUGBP1 RNA were incubated with (CUG)60. Fig. 3D shows that R2 region, which contained the CAG rich region (see Fig. 3A), produced a band shift. To confirm that these band shifts were produced by the formation of double strand RNA (dsRNA), the incubations were processed by Rnase III diluted to either 0.0001, 0.001 or 0.01 U. Fig. 3E shows that the band shifts disappeared as the concentrations of Rnase III were increased. Finally, we diluted the CUGBP1 RNA to 20, 40, 60, 80, 100 and 120 pM with RNase free water, and added 20 pM of (CUG)60 RNA. Fig. 3F shows that an 80 pM concentration of CUGBP1 RNA was required for the band of (CUG)60 RNA to disappear.

4. Discussion

In this study, we performed differential display analysis to find mRNAs whose levels of expression are altered in muscle tissue of DM1 patients. We showed that CUGBP1 mRNA levels were lower in DM1 patients compared to those in normal individuals and myopathic disease controls. Furthermore, the amount of the mRNA was demonstrated to negatively correlate with the number of CTG repeats. From these results, we speculated that the mutant expansion may be involved in the alteration of CUGBP1 mRNA expression.

The repeat expansion has been suggested to affect neighboring DNAs located on chromosome 19q 13.3, such as the DMAHP gene, which is present in the 3′ untranslated region of the DMPK gene (Thornton et al., 1997; Klesert et al., 1997), or *dmwd*, a gene upstream of the DMPK start site (Eriksson et al., 1999). However, these observations may not be identical to our results, since the CUGBP1 gene is located in chromosome 11p11.

The CTG expansion has been reported to alter the accumulation of poly(A) + RNA in *trans* in DM1 muscle biopsies (Wang et al., 1995). Several studies have demonstrated that the expression of specific mRNAs is affected in DM1 patients. For example, insulin receptor mRNA is reduced in DM1 biopsy specimens (Morrone et al., 1997). In addition, the expression of ion channel mRNAs is altered in DM1 muscle (Kimura et al., 2000), and the expression of muscle-specific chloride channel mRNA is altered in a transgenic mouse model (Charlet et al., 2002) and in DM1 patients (Charlet et al., 2002; Mankodi et al., 2002). The mechanism by which the expression of particular genes is affected in DM1 patients remains unknown. It was reported that mutant CUG expansion has base-pairing interaction with other mRNAs that have expanded CAG repeats in vitro (Sasagawa et al., 1999). The authors reported that the RNA–RNA complex forms when the number of CUG and

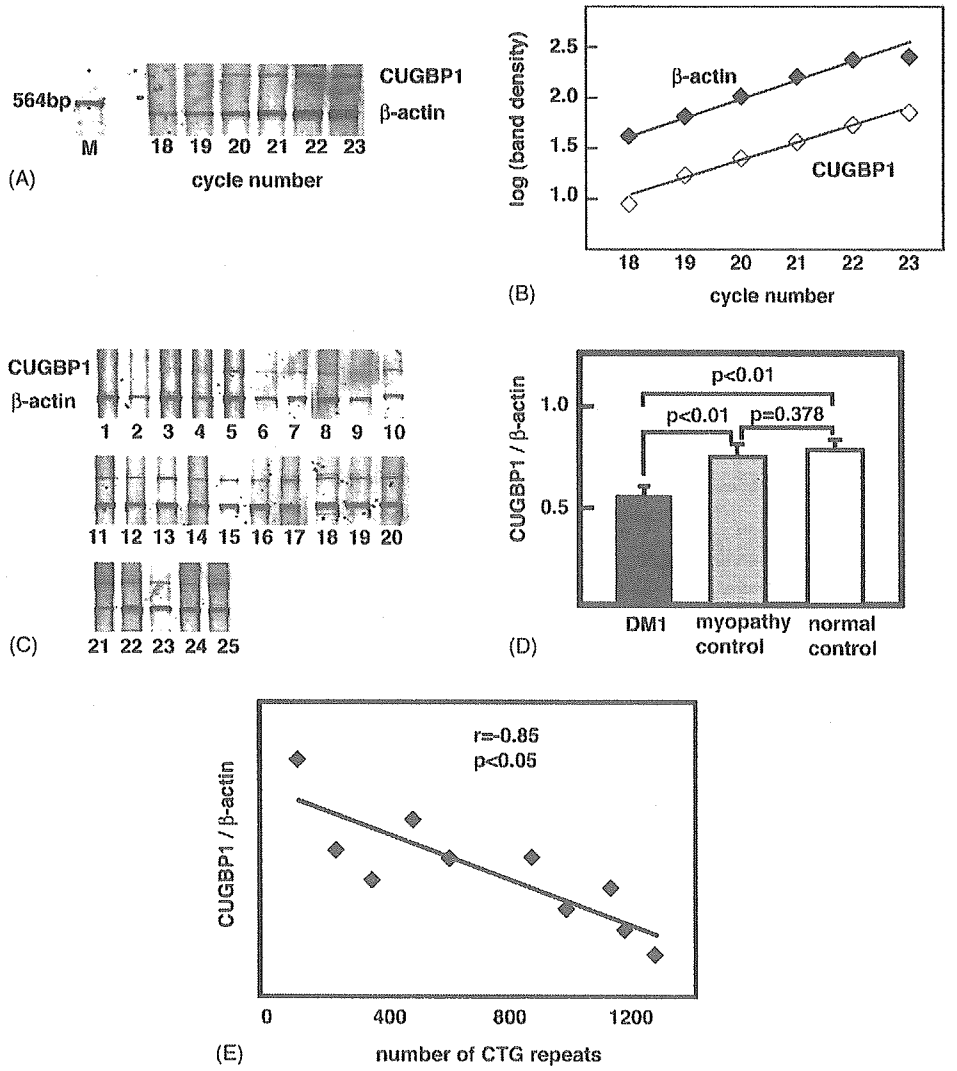

Fig. 2. Measurement of the CUGBP1 mRNA by semi-quantitative multiplex PCR assay. Reactions were sampled at every cycle of reaction, resolved by electrophoresis on 5% polyacrylamide sequencing gel and stained with SYBR Green I (A). Reaction cycle-intensity curves are fitted to the linear portion of a semi-logarithmic graph between 18 and 23 cycles, and it is assumed that both PCR products would be amplified with comparable efficiency under those conditions (B). (C) Gel images of the multiplex PCR with tissue expression levels of β-actin and CUGBP1 mRNAs. The numbers below the gel photograph are 1–10: DM1 patients; 11–20: myopathic controls; and 21–25: normal controls. (D) Differences in the ratio of CUGBP1 to β-actin band density between DM1 and controls. (E) Correlation of the number of CTG repeats with the relative band density in DM1 patients.

CAG repeats is over 140 and 35, respectively. However, in present study, (CUG)60 hybridized with (CAG)12, as well as with (CAG) These discrepancies may be caused by differences in the experimental procedures. In the previous study, RNAs were generated in a same tube and hybridized without heating, while, in the present study, we generated RNAs in separate tubes and heated the samples, followed by hybridization (see methods). We demonstrated that CUGBP1 RNA, which has short CAG repeats sequences, hybridized with (CUG)60, despite the fact that it did not bind to (CUG) These results suggest that the expanded CUG repeat may interact with complementary CAG repeat sequences within the CUGBP1 mRNA. This possibility is supported by the present data that the CUG expansion did not bind to β-actin RNA and CUGBP1 anti-sense RNA, which have no CAG repeats within their PCR-amplified sequences.

Fig. 3B showed slight band shifts in all lanes that contain more than one RNA in addition to those indicated by closed arrow heads. Since relatively smaller band shifts do not necessarily indicate that they have weaker interaction, we did negative control experiments using (CUG)12 RNA probe for Figs. 3E and F. To clarify whether this band shift is derived from formation of (CUG)12-CUGBP1 complex, we performed RNase III protection assay. We found that band pattern including the band shift was not changed after incubation with 0.01 Unit RNase III at 37 °C for 15 min, although intensities of each band corresponding to CUGBP1 and (CUG)12 were slightly increased (data not shown). Next, to examine the dose-dependent synthesis of RNA–RNA

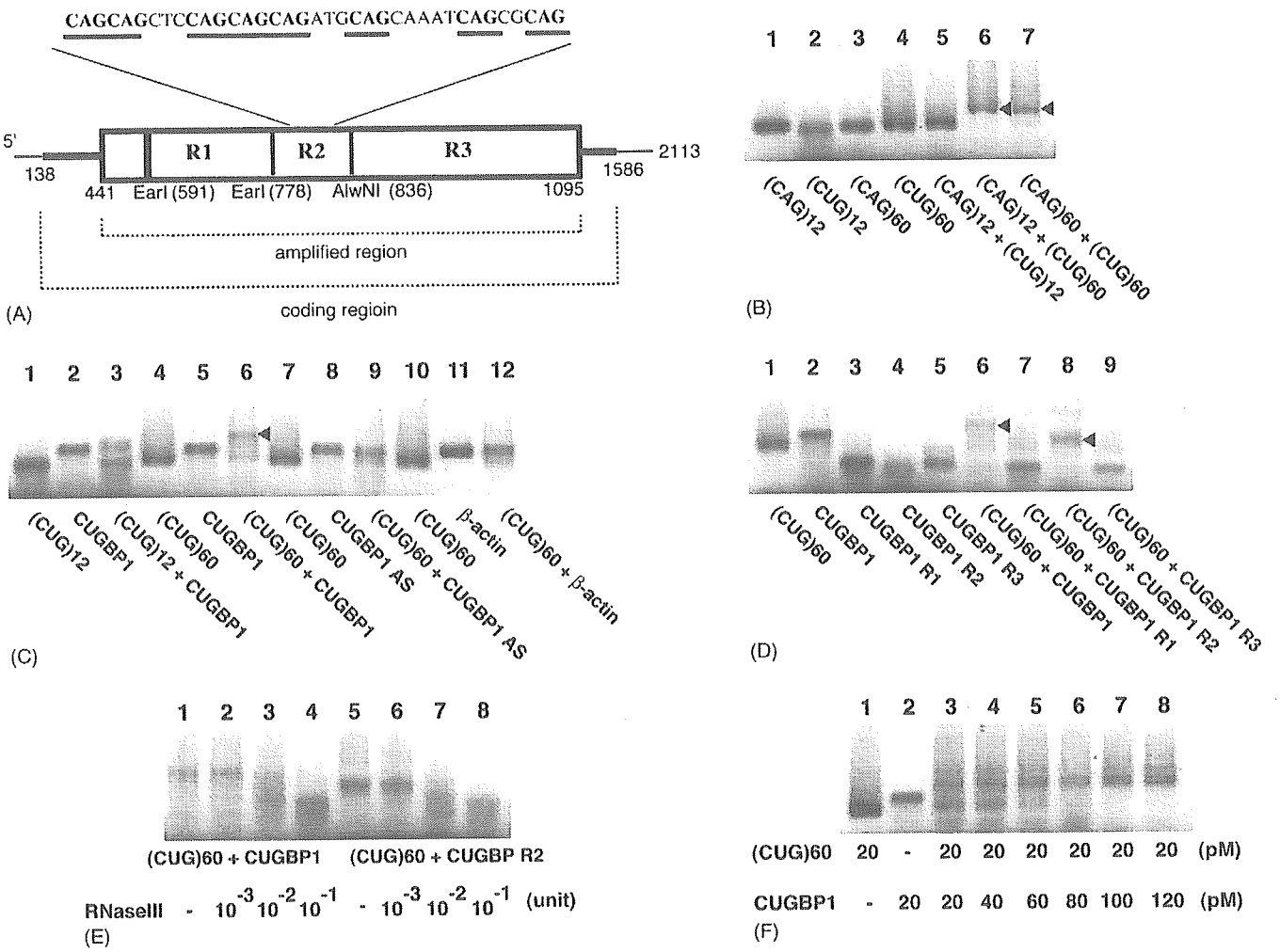

Fig. 3. In vitro binding of the RNA CUG repeat to CUGBP1 mRNA. (A) Whole molecule of CUGBP1 cDNA (Accession no. U63289), its coding sequence (138–1586nt) and PCR-amplified 655 bp product (441–1095nt). The product was cleaved with Ear I (position 591 and 778) and AlwNI (position 836) into three fragments, named R1 (591–778nt), R2 (778–836nt) and R3 (836–1095nt). CAG trinucleotides in R2 are underlined. (B) Antisense binding of CUG repeats to CAG repeats. Lane1, (CAG)12; lane2, (CUG)12; lane3, (CAG)60; lane4, (CUG)60; lane5, (CAG)12 + (CUG)12; lane6, (CAG)12 + (CUG)60; and lane7, (CAG)60 + (CUG)60. Band shifts are marked by an arrowhead. (C) Binding of CUG repeats to CUGBP1 RNA. Lane1, (CUG)12; lane2 and 5, CUGBP1 RNA; lane4, 7 and 10, (CUG)60; lane8, CUGBP1 anti-sense (AS) RNA; lane11, β-actin RNA; lane3, (CUG)12 + CUGBP1 RNA; lane6, (CUG)60 + CUGBP1 RNA; lane9, (CUG)60 + CUGBP1 anti-sense RNA; and lane12 (CUG)60 + β-actin RNA. Band shift is produced by the hybridization of (CUG)60 with CUGBP1 RNA (lane6, arrow head). (D) Binding of CUG repeats to the CAG rich region within CUGBP1 RNA. Lane1, (CUG)60; lane2, CUGBP1 RNA; lane3, CUGBP1 R1; lane4, CUGBP1 R2; lane5, CUGBP1 R3; lane6, (CUG)60 + CUGBP1 RNA; lane7, (CUG)60 + R1; lane8, (CUG)60 + R2; and lane9, (CUG)60 + R3. Band shift is seen in lane 8, as well as lane 6 (arrow head). (E) Degradation of hybrid RNAs by Rnase III. Lanes 1–4, (CUG)60 + CUGBP1 RNA; and lanes 5–8, (CUG)60 + CUGBP1 R2. Lanes 2–4 and 6–8 are incubations with RNase III at the indicated concentration. (F) Dose dependent synthesis in RNA–RNA complex. Lane1, (CUG)60; lane2, CUGBP1 RNA; and lane 3–8, (CUG)60 + CUGBP1 RNA. The concentrations of CUGBP1 RNAs in lanes 3–7 are 20, 40, 60, 80, 100 and 120 pM, respectively, and those of (CUG)60 were all 20 pM.

complex, we added 20 pM of (CUG)12 to 5, 10, 20, 30, 40 and 50 pM of CUGBP1 RNA, although we did not find significant change in the band intensity (data not shown). From these results, we suggested that CUGBP1 and (CUG)12 did not produce RNA–RNA complex. We suggest that a slight band shift may be largely caused by *cis*-effect within RNA. We also did the negative control studies using other RNA combinations, which were (CAG)12-(CUG)12, (CUG)60-CUGBP1(AS), (CUG)60-β-actin, (CUG)60-CUGBP1(R1) and (CUG)60-CUGBP1(R3), and we obtained the same results as that of (CUG)12-CUGBP1.

We showed that 20 pM of (CUG)60 RNA combined with 80 pM of CUGBP1 RNA in vitro. These observations suggest that as the size of the CUG expansion increases, it is able to interact with an increasing number of CUGBP1 mRNA molecules, which may explain the in vivo results that the expression of CUGBP1 mRNA correlated inversely with the number of CTG repeats in DM1 patients.

The biological effect of the RNA–RNA complex has not been fully clarified. Sasagawa et al. speculated that CUG/CAG double strand RNA may be recognized by a specific RNase and digested (Sasagawa et al., 1999). Our